

Multi-Boundary Entanglement in Chern-Simons Theory and Link Invariants

Vijay Balasubramanian^{1,2}, Jackson R. Fliss³, Robert G. Leigh³ and Onkar Parrikar¹

¹ *David Rittenhouse Laboratory, University of Pennsylvania, 209 S.33rd Street, Philadelphia PA, 19104, U.S.A.*

² *Theoretische Natuurkunde, Vrije Universiteit Brussel (VUB), and
International Solvay Institutes, Pleinlaan 2, B-1050 Brussels, Belgium*

³ *Department of Physics, University of Illinois, 1110 W. Green Street, Urbana IL, 61801, U.S.A.*

March 10, 2022

Abstract

We consider Chern-Simons theory for gauge group G at level k on 3-manifolds M_n with boundary consisting of n topologically linked tori. The Euclidean path integral on M_n defines a quantum state on the boundary, in the n -fold tensor product of the torus Hilbert space. We focus on the case where M_n is the link-complement of some n -component link inside the three-sphere S^3 . The entanglement entropies of the resulting states define framing-independent link invariants which are sensitive to the topology of the chosen link. For the Abelian theory at level k ($G = U(1)_k$) we give a general formula for the entanglement entropy associated to an arbitrary $(m|n-m)$ partition of a generic n -component link into sub-links. The formula involves the number of solutions to certain Diophantine equations with coefficients related to the Gauss linking numbers (mod k) between the two sublinks. This formula connects simple concepts in quantum information theory, knot theory, and number theory, and shows that entanglement entropy between sublinks vanishes if and only if they have zero Gauss linking (mod k). For $G = SU(2)_k$, we study various two and three component links. We show that the 2-component Hopf link is maximally entangled, and hence analogous to a Bell pair, and that the Whitehead link, which has zero Gauss linking, nevertheless has entanglement entropy. Finally, we show that the Borromean rings have a “W-like” entanglement structure (i.e., tracing out one torus does *not* lead to a separable state), and give examples of other 3-component links which have “GHZ-like” entanglement (i.e., tracing out one torus *does* lead to a separable state).

1 Introduction

An important open question in quantum mechanics and quantum information theory is to understand the possible patterns of entanglement that can arise naturally in field theory. The local structure of wavefunctions is typically determined largely by the locality of physical Hamiltonians because interactions create entanglement. However, entanglement is a global property and very little is known about how it can be organized over long distances. One way of thinking about this is to consider multiple disjoint regions that are sufficiently separated so that locality by itself will not prescribe the structure of entanglement. A challenge is that there is no general prescription for even classifying the patterns of entanglement between multiple disjoint entities. For three qubits, up to local operations, or more precisely up to SLOCC (Stochastic Local Operations and Classical Communication) transformations of the state, there are precisely two non-trivial classes of multipartite entanglement [1] – the GHZ class, represented by the state $(|111\rangle + |000\rangle)/\sqrt{2}$, has the property that tracing over one qubit disentangles the state, while in the W class, represented by $(|100\rangle + |010\rangle + |001\rangle)/\sqrt{3}$, a partial trace still leaves an entangled state of two qubits. A similar analysis of entanglement classes is not known in general for n qubits, or in the more physical case of LOCC equivalence, let alone for disjoint regions of a field theory.

Recently the AdS/CFT correspondence was proposed as a tool for studying multi-partite entanglement. The authors of [2,3] examined the multi-boundary three-dimensional wormhole solutions of [4–10] and found non-trivial entanglement, computed through the holographic Ryu-Takayangi formula [11], between subsets of boundary components. One interesting result was that although there were regions of parameter space where the entanglement between boundaries was entirely multi-partite, it was never of the GHZ type. In special limits it was also possible to analyze the structure of the CFT wavefunction in terms of the OPE coefficients. However, it was difficult to carry out a computation of entanglement entropies in the field theory at a generic point in the parameter space.

While the field theory calculation of multi-boundary entanglement entropies is difficult in general, one simple case where this can be done is in a topological quantum field theory [12–14] defined on a manifold M_n , with boundary Σ_n consisting of a union of n disjoint components $\{\sigma_1, \sigma_2, \dots, \sigma_n\}$. The Euclidean path integral for this theory as a functional of data on the boundary defines a wavefunction on Σ_n . This wavefunction is defined on the tensor product of Hilbert spaces \mathcal{H}_i associated with the different boundary components. Because the theory is topological there will be no local dynamics, and all of the entanglement arises from the topological properties of M_n . This allows us to focus attention on global features of entanglement, and we can hope that geometric and topological tools will come to our aid.

Here, we explore these ideas in the context of Chern-Simons gauge theories in three dimensions (see [12, 15] and references therein). Bi-partite entanglement of connected spatial sections in such theories was studied in [16–18]. By contrast, we consider Chern-Simons theory for group G at level k defined on 3-manifolds M_n with disconnected boundaries, namely n linked tori. More precisely, we will choose M_n to be link complements (see definition below) of n -component links in S^3 ; the wavefunctions on the tori in this case can be explicitly written in terms of *coloured link invariants*. For $G = U(1)_k$ this leads to a general formula for the entanglement entropy of any bipartition of the link into sub-links. Further, the entropy vanishes if and only if the Gauss linking number vanishes (modulo k) between the sub-links in the bipartition. It is also possible to construct states with non-zero tripartite mutual information of both signs. For $G = SU(2)_k$ we explicitly calculate entanglement entropies for a variety of 2- and 3-component links, and show that: (a) the Hopf link is the analog of a maximally-entangled Bell pair, (b) while the $U(1)$ entanglement is only sensitive to the Gauss linking number, the non-Abelian entanglement also detects more subtle forms of topology, and (c) GHZ-like states and W-like states are both realizable in terms of links with different topologies. Overall, multi-boundary entanglement entropy in Chern-Simons theory computes a framing-independent link invariant with physical motivation, and hence gives a potentially powerful tool for studying knots and links. Additionally, this setup also gives a calculable arena for the study of multi-partite entanglement.

Interestingly, at the classical level the three-dimensional theories of gravity studied in the holographic approach to multi-partite entanglement [2, 3] can themselves be written as Chern-Simons theories of the group $SL(2, R) \times SL(2, R)$. While it is not clear that 3d quantum gravity is entirely described by Chern-Simons theory [19], it is intriguing to speculate that we could use our Chern-Simons techniques to directly compute entanglement in three dimensional gravity.

The rest of the paper is organized as follows: in Section 2, we will construct the multi-boundary states we are interested in, and review some concepts required for later calculations. In Section 3, we will consider Chern-Simons theory for $G = U(1)_k$, and compute the entanglement entropy for a bi-partition of a generic n -component link into sub-links. In Section 4, we will consider multi-boundary entanglement in $G = SU(2)_k$ Chern-Simons. Here we will study several examples of two and three-component links and try to extract general lessons from these examples. Finally, we end with a discussion of open questions and future work in Section 5.

2 Multi-boundary States in Chern-Simons theory

We consider Chern-Simons theory with gauge group G at level k . The action of the theory on a 3-manifold M is given by

$$S_{CS}[A] = \frac{k}{4\pi} \int_M \text{Tr} \left(A \wedge dA + \frac{2}{3} A \wedge A \wedge A \right), \quad (1)$$

where $A = A_\mu dx^\mu$ is a gauge field (or equivalently, a connection on a principle G -bundle over M). The equation of motion corresponding to the above action is

$$F = dA + A \wedge A = 0. \quad (2)$$

Since the equation of motion restricts the phase space to flat connections (modulo gauge transformations), the only non-trivial, gauge invariant operators in the theory are *Wilson lines* along non-contractible cycles in M :

$$W_R(L) = \text{Tr}_R \mathcal{P} e^{i \oint_L A}, \quad (3)$$

where R is a representation of G , L is an oriented, non-contractible cycle in M and the symbol \mathcal{P} stands for path-ordering along the cycle L . If M has a boundary Σ , then the path-integral of the theory on M with Wilson line insertions, and boundary conditions $A|_\Sigma = A^{(0)}$ imposed on Σ ,¹ namely

$$\Psi_{(R_1, L_1), \dots, (R_n, L_n)}[A^{(0)}] = \int_{A|_\Sigma = A^{(0)}} [DA] e^{i S_{CS}[A]} W_{R_1}(L_1) \cdots W_{R_n}(L_n) \quad (4)$$

is interpreted as the wavefunction of a state in the Hilbert space $\mathcal{H}(\Sigma; G, k)$ which Chern-Simons theory associates to Σ . In this paper, we consider states in the n -fold tensor product $\mathcal{H}^{\otimes n}$, where $\mathcal{H} = \mathcal{H}(T^2; G, k)$ is the Hilbert space of Chern-Simons theory for the group G at level k on a torus. These states can be understood as being defined on n copies of T^2 , namely the spatial manifold Σ_n

$$\Sigma_n = \amalg_{i=1}^n T^2, \quad (5)$$

where \amalg denotes disjoint union (see Figure 1). A natural way to construct states in a QFT is by performing the Euclidean path integral of the theory on a 3-manifold M_n whose boundary is $\partial M_n = \Sigma_n$. In a general field theory the state constructed in this way will depend on the detailed geometry of M_n , for instance the choice of metric on M_n , but in our situation only the topology of M_n matters. However, there are many topologically distinct Euclidean 3-manifolds with the same boundary, and the path integrals on these manifolds will construct different states on Σ_n . We will focus on a simple class of such 3-manifolds, which we will now describe.

¹When M has a boundary, then the action must be augmented by including certain boundary terms, which correspond to picking a Lagrangian submanifold in phase space. We will not need to dwell on these details in the present paper.

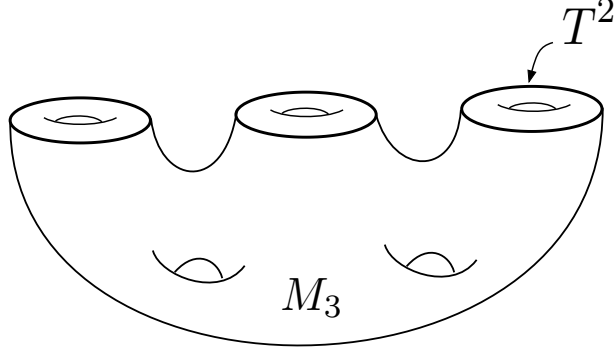


Figure 1: The spatial manifold Σ_n for $n = 3$ is the disjoint union of three tori. M_n is a 3-manifold such that $\partial M_n = \Sigma_n$.

We start with a connected, closed 3-manifold (i.e., a connected, compact 3-manifold without boundary) X . An n -component *link* in X is an embedding of n (non-intersecting) circles in X . (Note that 1-component links are conventionally called *knots*.) We will sometimes use Rolfsen notation to denote a link \mathcal{L} as $\mathcal{L} = c_m^n$, where c is the number of crossings, n is the number of components in the link, and m is the chronological rank at which the link is presented in the Rolfsen table [20] for a given c and n . We will sometimes merely denote a generic n -component link as \mathcal{L}^n , when we do not need to choose a particular link. We will label the n circles which constitute the link as L_1, \dots, L_n , so $\mathcal{L}^n = L_1 \cup L_2 \cup \dots \cup L_n$. Now in order to construct the desired 3-manifold M_n , we pick a link \mathcal{L}^n in X and *drill* out a tubular neighbourhood $\tilde{\mathcal{L}}^n$ of the link in S^3 . In other words, we take M_n to be the complement of \mathcal{L}^n in X , i.e., $M_n = X - \tilde{\mathcal{L}}^n$ (see Figure 2). This is a standard construction; the 3-manifold M_n we have obtained starting from X and \mathcal{L}^n is called the *link complement* of \mathcal{L}^n in X . Since \mathcal{L}^n is an n -component link, its link complement M_n is a manifold with precisely the desired boundary

$$\partial M_n = \coprod_{i=1}^n T^2. \quad (6)$$

We can therefore perform the path-integral of Chern-Simons theory on M_n , and obtain a state on Σ_n . In fact, *every topological 3-manifold M_n which has the disjoint union of n tori as its boundary, is a link-complement $X - \mathcal{L}^n$, for some closed 3-manifold X and an n -component link \mathcal{L}^n in X* . This construction assigns a state $|\mathcal{L}^n, X\rangle$ to every pair (X, \mathcal{L}^n) – we will sometimes refer to these states as *link states*. In this paper, we will focus on the class of states constructed this way, but where we take X to be the 3-sphere S^3 .

To further understand the state $|\mathcal{L}^n, S^3\rangle$, or simply $|\mathcal{L}^n\rangle$ for short, we need to know some details about the Hilbert space of Chern-Simons theory on a torus T^2 [12]. Let us picture the 2-torus as the boundary of a solid torus inside S^3 (see Figure 3). We pick two simple cycles on the torus which generate its fundamental group and label them \mathbf{m} and ℓ , with \mathbf{m} being the *meridian*, i.e., contractible inside the solid torus. The choice of ℓ , called the *longitude*, is not unique. But let

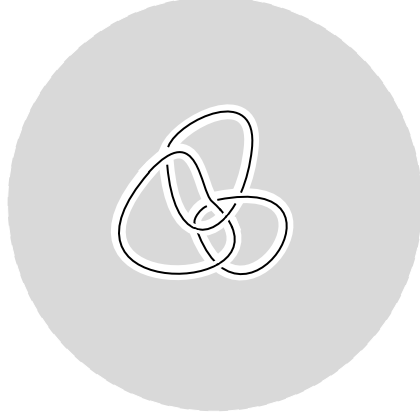


Figure 2: The link complement (the shaded region) of a 3-component link (bold lines) inside the three-sphere. The white region indicates a tubular neighbourhood of the link which has been drilled out of the 3-sphere.

us make the canonical choice for ℓ , namely the one which is contractible in the complement of the torus inside S^3 ; we will later return to this point, which is related to *framing*. In order to construct a basis for the Hilbert space $\mathcal{H}(T^2; G, k)$ we perform the Chern-Simons path integral on the solid torus with a Wilson line in the representation R_j placed in the bulk of the solid torus running parallel to the longitude cycle ℓ , where the index j denotes an *integrable* representation of the gauge group G at level k . This gives a state on T^2 which we call $|j\rangle$. The conjugate of this state $\langle j|$ can be thought of in terms of the path integral on the solid torus with a Wilson line in the conjugate representation R_j^* . By letting j run over all the integrable representations [21] of G , we obtain a basis for the torus Hilbert space. Notably, the Hilbert space \mathcal{H} obtained in this way is finite dimensional. For example if we take $G = SU(2)_k$, the integrable representations are labelled by their spin j for $j = 0, \frac{1}{2}, \dots, \frac{k}{2}$, and so $\dim(\mathcal{H}(T^2; SU(2), k)) = k + 1$. Similarly in $G = U(1)_k$, the allowed representations are labeled by integer-valued charges $0 \leq q < k$, and so $\dim(\mathcal{H}(T^2; U(1), k)) = k$. We also note that the modular group $SL(2, \mathbb{Z})$ of large diffeomorphisms of the torus, generated by

$$\mathcal{T} : \tau \rightarrow \tau + 1, \quad \mathcal{S} : \tau \rightarrow -\frac{1}{\tau} \quad (7)$$

acts naturally on $\mathcal{H}(T^2; G, k)$. For example in the $U(1)_k$ theory, these operators take the following simple form [18] in the basis we introduced above²:

$$\mathcal{T}_{q_1, q_2} = e^{2\pi i h_{q_1}} \delta_{q_1, q_2}, \quad \mathcal{S}_{q_1, q_2} = \frac{1}{\sqrt{k}} e^{\frac{2\pi i q_1 q_2}{k}} \quad (8)$$

where $h_q = q^2/2k$. Similarly, for $SU(2)_k$ we have

$$\mathcal{T}_{j_1, j_2} = e^{2\pi i h_{j_1}} \delta_{j_1, j_2}, \quad \mathcal{S}_{j_1, j_2} = \sqrt{\frac{2}{k+2}} \sin\left(\frac{\pi(2j_1+1)(2j_2+1)}{k+2}\right) \quad (9)$$

²The \mathcal{T} matrices generally also contain an additional overall phase proportional to the central charge; we have omitted this phase above since it will not play any role in our discussion.

where $h_j = \frac{j(j+1)}{k+2}$. It is not hard to check that these matrices satisfy the relations $\mathcal{S}^2 = 1$ and $(\mathcal{ST})^3 = 1$.

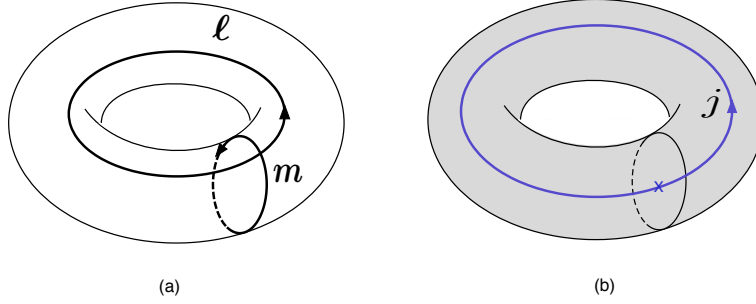


Figure 3: (a) The meridian and longitude cycles on a torus T^2 . (b) The state $|j\rangle$ corresponds to a Wilson line in the representation j placed in the bulk of the solid torus.

Now let us write the state $|\mathcal{L}^n\rangle \in \mathcal{H}^{\otimes n}$ obtained by performing the path-integral of Chern-Simons theory on the link complement of the link \mathcal{L}^n in terms of the above basis vectors:

$$|\mathcal{L}^n\rangle = \sum_{j_1, \dots, j_n} C_{\mathcal{L}^n}(j_1, j_2, \dots, j_n) |j_1, j_2, \dots, j_n\rangle, \quad |j_1, j_2, \dots, j_n\rangle \equiv |j_1\rangle \otimes |j_2\rangle \otimes |j_n\rangle \quad (10)$$

where $C_{\mathcal{L}^n}(j_1, \dots, j_n)$ are complex coefficients, which we can write explicitly as

$$C_{\mathcal{L}^n}(j_1, j_2, \dots, j_n) = \langle j_1, j_2, \dots, j_n | \mathcal{L}^n \rangle. \quad (11)$$

Operationally, this corresponds to gluing in solid tori along the boundary of the link complement $S^3 - \mathcal{L}^n$, but with Wilson lines in the representation $R_{j_i}^*$ placed in the bulk of the i^{th} torus. Thus, the coefficients $C_{\mathcal{L}^n}(j_1, \dots, j_n)$ are precisely the *coloured link invariants* of Chern-Simons theory with the representation $R_{j_i}^*$ placed along the i^{th} component of the link:

$$C_{\mathcal{L}^n}(j_1, \dots, j_n) = \left\langle W_{R_{j_1}^*}(L_1) \cdots W_{R_{j_n}^*}(L_n) \right\rangle_{S^3}, \quad (12)$$

where we recall that L_i are the individual circles which constitute the link, namely $\mathcal{L}^n = L_1 \cup \dots \cup L_n$. Thus, the link state $|\mathcal{L}^n\rangle$ encodes all the coloured link invariants corresponding to the link \mathcal{L}^n at level k .

We are interested in studying the entanglement structure of these states. To do so, we will compute the entanglement entropy corresponding to partitioning the n -component link into an m -component sub-link $L_1 \cup L_2 \cup \dots \cup L_m$ and its complement $L_{m+1} \cup \dots \cup L_n$

$$S_{EE; (L_1, \dots, L_m | L_{m+1}, \dots, L_n)} = -\text{Tr}_{L_{m+1}, \dots, L_n}(\rho \ln \rho), \quad \rho = \frac{1}{\langle \mathcal{L}^n | \mathcal{L}^n \rangle} \text{Tr}_{L_1, \dots, L_m} |\mathcal{L}^n\rangle \langle \mathcal{L}^n|, \quad (13)$$

where by tracing over L_i we mean tracing over the Hilbert space of the torus boundary corresponding to the circle L_i . We will interchangeably use the notation $(L_1, \dots, L_m | L_{m+1}, \dots, L_n)$ or $(m | n - m)$

to denote such bi-partitions; the former notation makes explicit which components of the link will be traced over.

This computation can be carried out generally in the case of $G = U(1)_k$; we do this in Section 3. In the non-Abelian case (we take $G = SU(2)_k$ for simplicity), the general computation is more challenging, and so we will proceed by considering various examples of two- and three-component links in Section 4. This will help us extract useful lessons about the topological entanglement structure of these link states.

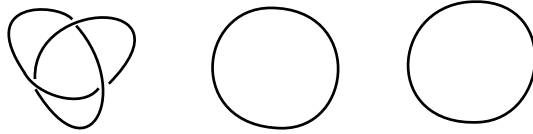


Figure 4: Three unlinked knots.

However, two important facts are immediately obvious:

- Take the link \mathcal{L}^n to be n un-linked knots (see Figure 4). In this case, it is well-known that the coloured link-invariant in equation (12) factorizes:

$$\frac{C_{\text{unlink}}(j_1, \dots, j_n)}{C_0} = \prod_{i=1}^n \frac{C_{L_i}(j_i)}{C_0} \quad (14)$$

where $C_0 = \mathcal{S}_0^0$ is the partition function of Chern-Simons theory on S^3 . It is then clear that the state $|\mathcal{L}^n\rangle$ is a product state

$$|\mathcal{L}^n\rangle \propto |L_1\rangle \otimes |L_2\rangle \otimes \dots \otimes |L_n\rangle \quad (15)$$

and hence the state $|\mathcal{L}^n\rangle$ is completely unentangled. This is our first hint that the quantum entanglement of link states captures aspects of the topology of the corresponding links. Specifically, *quantum entanglement of a bipartition of \mathcal{L}^n into two components implies topological linking between the two sub-links*. For $U(1)_k$ Chern-Simons theory we will also prove a converse in the next section (in terms of Gauss linking), but we have not yet arrived at a proof for general non-Abelian theories.

- Above, we ignored the issue of *framing* [12] of the individual circles comprising the link \mathcal{L}^n . Intuitively, if we replace each of the circles in the link with a ribbon, then the relative linking number between the two edges of the ribbon, or *self-linking*, is ambiguous. In general, to fix this ambiguity we must pick a framing for each circle, and consequently the coloured link invariants are really defined for framed links. However a different choice of framing of, let's say, the i^{th} circle L_i by t units is equivalent to performing a t -fold Dehn twist on the

corresponding torus. This corresponds to a local unitary transformation on the corresponding link state:

$$|\mathcal{L}^n\rangle \rightarrow (1 \otimes 1 \cdots \otimes \mathcal{T}_i^t \otimes 1 \cdots \otimes 1) |\mathcal{L}^n\rangle \quad (16)$$

where \mathcal{T}_i is a Dehn-twist on the i^{th} torus. Local unitary transformations of this type do not affect the entanglement entropies we are interested in. Hence, *the entanglement entropies are framing-independent link invariants.*

3 The Abelian case: $G = U(1)_k$

In this section we will compute the entanglement entropy for arbitrary bi-partitions of a generic n -component link in $U(1)_k$ Chern-Simons theory. As warm-up, we will start with two-component links, and then build up to the general case.

3.1 Two-component links

The main result we will use throughout this section is that if we have an n -component link \mathcal{L}^n with charges q_1, q_2, \dots, q_n placed on the circles L_1, L_2, \dots, L_n respectively, then the corresponding coloured link invariant in $U(1)_k$ Chern-Simons theory is given by [12]

$$C_{\mathcal{L}^n}(q_1, q_2, \dots, q_n) \equiv \langle W_{-q_1}(L_1) \cdots W_{-q_n}(L_n) \rangle_{S^3} = \exp \left(\frac{2\pi i}{k} \sum_{i < j} q_i q_j \ell_{ij} \right) \quad (17)$$

where ℓ_{ij} is the Gauss linking number between the circles L_i and L_j . When $i = j$, this is interpreted as the self-linking or framing of L_i . We will pick $\ell_{ii} = 0$ by convention, which is reflected in the above summation. However, as discussed in the previous section, the entanglement entropies we compute are independent of the choice of ℓ_{ii} . We note from equation (17) that the $C_{\mathcal{L}^n}$ remains unchanged under shifts by multiples of k : $\ell_{ij} \rightarrow \ell_{ij} + \mathbb{Z}k$. We will therefore assume that the ℓ_{ij} are all chosen such that $0 \leq \ell_{ij} < k$, i.e., $\ell_{ij} \in \mathbb{Z}_k$.

For a two component link \mathcal{L}^2 , equation (17) then implies that the wavefunction is

$$|\mathcal{L}^2\rangle = \frac{1}{k} \sum_{q_1, q_2} e^{\frac{2\pi i q_1 q_2}{k} \ell_{12}} |q_1\rangle \otimes |q_2\rangle \quad (18)$$

where the sum runs over 0 to $k - 1$, i.e., \mathbb{Z}_k , and we have introduced a factor of k^{-1} above to normalize the state. If we now wish to compute the entanglement entropy between 1 and 2, the

first step is to trace out one of the links:

$$\rho_1 = \text{Tr}_{L_2} |\mathcal{L}^2\rangle\langle\mathcal{L}^2| = \frac{1}{k^2} \sum_{q_1, q'_1, p} |q_1\rangle\langle q'_1| e^{2\pi i \frac{(q_1 - q'_1)\ell_{12}}{k} p} \quad (19)$$

The sum over p is easy to perform, and we obtain

$$\frac{1}{k} \sum_{p=0}^{k-1} e^{2\pi i \frac{(q_1 - q'_1)\ell_{12}}{k} p} = \eta_{q_1, q'_1}(k, \ell_{12}) \equiv \begin{cases} 1 & \cdots & \ell_{12}(q_1 - q'_1) = 0 \pmod{k} \\ 0 & \cdots & \ell_{12}(q_1 - q'_1) \neq 0 \pmod{k} \end{cases} \quad (20)$$

The matrix $\eta_{q_1, q'_1}(k, \ell_{12})$ can be written in the following tensor-product form

$$\eta(k, \ell_{12}) = \begin{pmatrix} 1 & 1 & \cdots & 1 \\ 1 & 1 & \cdots & 1 \\ \vdots & \vdots & & \vdots \\ 1 & 1 & \cdots & 1 \end{pmatrix}_{(g, g)} \otimes \begin{pmatrix} 1 & 0 & \cdots & 0 \\ 0 & 1 & \cdots & 0 \\ \vdots & \vdots & & \vdots \\ 0 & 0 & \cdots & 1 \end{pmatrix}_{\left(\frac{k}{g}, \frac{k}{g}\right)} \quad (21)$$

where $g = \text{gcd}(k, \ell_{12})$ and the subscripts on the matrices indicate their dimensions. The eigenvalues of η are therefore $\lambda_1 = 0$ with degeneracy $\left(k - \frac{k}{\text{gcd}(k, \ell_{12})}\right)$, and $\lambda_2 = \text{gcd}(k, \ell_{12})$ with degeneracy $\frac{k}{\text{gcd}(k, \ell_{12})}$. Computing the entanglement entropy from here, we find

$$S_{EE; L_1|L_2}(\mathcal{L}^2) = \ln \left(\frac{k}{\text{gcd}(k, \ell_{12})} \right) \quad (22)$$

Thus the entanglement entropy in this case captures information about the Gauss linking number ℓ_{12} filtered by the level of the Chern-Simons theory, namely $\text{gcd}(k, \ell_{12})$. Note from the above formula that the Hopf link (which has $\ell_{12} = 1$) is maximally entangled – this is in fact generally true even in the non-Abelian case, as we will see later. *Thus, the Hopf link is analogous to a Bell pair in quantum information theory.*

For later use, it is useful to derive the above expression from a slightly different point of view, using Renyi entropies. The \mathbf{n} th Renyi entropy is defined as

$$S_{\mathbf{n}}(\mathcal{L}^2) = \frac{1}{1 - \mathbf{n}} \ln \text{Tr}_{L_1} \rho_1^{\mathbf{n}} \quad (23)$$

where \mathbf{n} is called the Renyi index and the subscript on the trace indicates that we are tracing over the first Hilbert space. The entanglement entropy is obtained as the limit $\mathbf{n} \rightarrow 1$. From equation (19), we obtain

$$S_{\mathbf{n}} = \frac{1}{1 - \mathbf{n}} \ln \left(\frac{1}{k^{\mathbf{n}}} \sum_{q_1, \dots, q_{\mathbf{n}}} \eta_{q_1, q_2}(k, \ell_{12}) \eta_{q_2, q_3}(k, \ell_{12}) \cdots \eta_{q_{\mathbf{n}}, q_1}(k, \ell_{12}) \right) \quad (24)$$

where all the sums are over \mathbb{Z}_k . The summand is non-zero only provided we satisfy the following conditions

$$\begin{aligned}\ell_{12}(q_1 - q_2) &= 0 \pmod{k} \\ \ell_{12}(q_2 - q_3) &= 0 \pmod{k} \\ &\vdots \\ \ell_{12}(q_n - q_1) &= 0 \pmod{k},\end{aligned}\tag{25}$$

in which case it is equal to one. So the sum in equation (24) is essentially the number of solutions inside \mathbb{Z}_k^n to the above equations. Suppose we pick an integer $0 \leq q_1 < k$. Then q_2 can take on $\gcd(k, \ell_{12})$ values such that the first of the above conditions is satisfied. Similarly, q_3 can take $\gcd(k, \ell_{12})$ values such that the second condition is satisfied, and so on. The last condition of course is redundant once we satisfy the first $n - 1$ of them. Finally, summing over q_1 , we obtain

$$S_n(\mathcal{L}^2) = \frac{1}{1-n} \ln \left(\frac{\gcd(k, \ell_{12})}{k} \right)^{n-1} = \ln \left(\frac{k}{\gcd(k, \ell_{12})} \right)\tag{26}$$

So we find that the Renyi entropies S_n are in fact independent of n . Thus the $n \rightarrow 1$ limit is trivial, and is equal to the entanglement entropy $S_{EE; L_1|L_2}$ computed previously. We will find that the above Renyi trick easier to work with in the general case.

3.2 Three-component links

Let us now move on to the case of 3-component states. Again, we take a generic 3-component link \mathcal{L}^3 and use the coloured link invariants to write down the corresponding state

$$|\mathcal{L}^3\rangle = \frac{1}{k^{3/2}} \sum_{q_1, q_2, q_3} e^{2\pi i \left(\frac{q_1 q_2}{k} \ell_{12} + \frac{q_2 q_3}{k} \ell_{23} + \frac{q_3 q_1}{k} \ell_{13} \right)} |q_1\rangle \otimes |q_2\rangle \otimes |q_3\rangle.\tag{27}$$

Let us consider the entanglement entropy for the bi-partition $(L_1|L_2, L_3)$. We trace out links 2 and 3 to obtain the reduced density matrix over the first factor:

$$\rho_1 = \text{Tr}_{L_2, L_3} |\mathcal{L}^3\rangle \langle \mathcal{L}^3| = \frac{1}{k} \sum_{q, q'} |q\rangle \langle q'| \eta_{q, q'}(k, \ell_{12}) \eta_{q, q'}(k, \ell_{13})\tag{28}$$

where η is the matrix in (21). Repeating the arguments in the two-component case, it is easy to show that the non-zero eigenvalue of the reduced density matrix is $\lambda = \frac{\gcd(k, \ell_{12}, \ell_{13})}{k}$ with degeneracy $\frac{k}{\gcd(k, \ell_{12}, \ell_{13})}$. Thus, the entanglement entropy is given by

$$S_{EE; L_1|L_2, L_3}(\mathcal{L}^3) = \ln \left(\frac{k}{\gcd(k, \ell_{12}, \ell_{13})} \right)\tag{29}$$

Let us now compute the Renyi entropies for the $(L_1|L_2, L_3)$ partition. From equations (23) and (28), we obtain

$$S_{\mathbf{n}}(\mathcal{L}^3) = \frac{1}{1 - \mathbf{n}} \ln \left(\frac{1}{k^{\mathbf{n}}} \sum_{q_1, \dots, q_n} \eta_{q_1, q_2}(k, \ell_{12}) \eta_{q_1, q_2}(k, \ell_{13}) \cdots \eta_{q_n, q_1}(k, \ell_{12}) \eta_{q_n, q_1}(k, \ell_{13}) \right) \quad (30)$$

Following arguments similar to the two-component case, the sum only receives contributions from terms which satisfy

$$\begin{aligned} \ell_{12}(q_1 - q_2) &= 0 \pmod{k}, & \ell_{13}(q_1 - q_2) &= 0 \pmod{k} \\ \ell_{12}(q_2 - q_3) &= 0 \pmod{k}, & \ell_{13}(q_2 - q_3) &= 0 \pmod{k} \\ &\vdots & & \\ \ell_{12}(q_n - q_1) &= 0 \pmod{k}, & \ell_{13}(q_n - q_1) &= 0 \pmod{k} \end{aligned} \quad (31)$$

where we note that the number of constraints has doubled as compared to the two-component case. The sum in equation (30) is then precisely equal to the number of integer-valued solutions in $\mathbb{Z}_k^{\mathbf{n}}$ to the congruences (31). To find these solutions, once again we pick some $0 \leq q_1 < k$. Then the number of choices for q_2 corresponds to the number of solutions to the equations

$$\ell_{12} x = 0 \pmod{k}, \quad \ell_{13} x = 0 \pmod{k}. \quad (32)$$

which is $\gcd(k, \ell_{12}, \ell_{13})$. Similarly, q_3 can be picked in $\gcd(k, \ell_{12}, \ell_{13})$ ways, and so on. Finally, summing over q_1 , we obtain

$$S_{\mathbf{n}}(\mathcal{L}^3) = \ln \left(\frac{k}{\gcd(k, \ell_{12}, \ell_{13})} \right) \quad (33)$$

which agrees with eq. (29). Once again, we note that the Renyi entropies are independent of the Renyi index \mathbf{n} .

It is useful to make the above counting procedure more systematic. Let us define the *linking matrix* for the $(L_1|L_2, L_3)$ partition as (the general definition is given below, eq. (42))

$$\mathbf{G} = \begin{pmatrix} \ell_{12} \\ \ell_{13} \end{pmatrix} \quad (34)$$

We interpret \mathbf{G} as a matrix over the field \mathbb{Z}_k , i.e., as a map $\mathbf{G} : \mathbb{Z}_k \rightarrow \mathbb{Z}_k \times \mathbb{Z}_k$. Then, the Renyi entropy, eq. (33), can be rewritten in terms of the linking matrix as

$$S_{\mathbf{n}} = \ln \left(\frac{k}{|\ker \mathbf{G}|} \right) \quad (35)$$

where by $|\ker \mathbf{G}|$ we mean the number of solutions in \mathbb{Z}_k to the congruences (32), *including* the zero solution. In the present case, clearly $|\ker \mathbf{G}| = \gcd(k, \ell_{12}, \ell_{13})$.

We can also compute other information theoretic quantities in this setup, for instance the *mutual information* between, say, the links L_1 and L_2

$$I(L_1, L_2) = S_{EE}(L_1) + S_{EE}(L_2) - S_{EE}(L_1 \cup L_2) = \ln \left(\frac{\gcd(k, \ell_{13}, \ell_{23})}{\gcd(k, \ell_{12}, \ell_{13}) \gcd(k, \ell_{12}, \ell_{23})} k \right) \quad (36)$$

where $S_{EE}(L_1) \equiv S_{EE; L_1 | L_2, L_3}$, $S_{EE}(L_2) \equiv S_{EE; L_2 | L_1, L_3}$, and $S_{EE}(L_1 \cup L_2) \equiv S_{EE; L_1, L_2 | L_3}$. A standard result in quantum information theory is that the mutual information is a positive semi-definite quantity. This positivity condition together with equation (29) then translates to the identity

$$\frac{\gcd(k, \ell_{12}, \ell_{13}) \gcd(k, \ell_{12}, \ell_{23})}{\gcd(k, \ell_{13}, \ell_{23})} \leq k \quad (37)$$

which is easily verified.

3.3 n -component links

Let us now consider an n -component link \mathcal{L}^n . We wish to compute the entanglement entropy for a $(m|n-m)$ bipartition between the m -component sublink consisting of the circles (L_1, L_2, \dots, L_m) and the complement sub-link consisting of (L_{m+1}, \dots, L_n) . We may choose $m \leq n-m$ without loss of generality. Tracing over the links (L_{m+1}, \dots, L_n) , we obtain the reduced density matrix:

$$\rho_{1,2,\dots,m} = \frac{1}{k^m} \sum_{q_1, \dots, q_m} \sum_{q'_1, \dots, q'_m} \left(\prod_{i=m+1}^n \eta_{q_1 \dots q_m; q'_1 \dots q'_m}(k, \ell_{1,i}, \ell_{2,i}, \dots, \ell_{m,i}) \right) e^{i\phi} |q_1 \dots q_m\rangle \langle q'_1, \dots, q'_m| \quad (38)$$

where

$$\eta_{q_1, \dots, q_m; q'_1, \dots, q'_m}(k, \ell_{1,i}, \dots, \ell_{m,i}) = \frac{1}{k} \sum_p e^{\frac{2\pi i}{k} ((q_1 - q'_1)\ell_{1,i} + (q_2 - q'_2)\ell_{2,i} + \dots + (q_m - q'_m)\ell_{m,i})p}, \quad (39)$$

and

$$e^{i\phi} = e^{\frac{2\pi i}{k} \sum_{i < j}^m (q_i q_j - q'_i q'_j) \ell_{ij}} \quad (40)$$

is an unimportant phase which can be eliminated by a unitary transformation on $L_1 \cup L_2 \dots \cup L_m$ (such unitaries acting only on one side of the bi-partition do not affect the entanglement entropy).

Using precisely the same arguments as before, we can compute the Renyi entropy and we find

$$S_n(\mathcal{L}^n) = \ln \left(\frac{k^m}{|\ker \mathbf{G}|} \right), \quad (41)$$

where \mathbf{G} here is the appropriate linking matrix across the $(m|n-m)$ -partition,

$$\mathbf{G} = \begin{pmatrix} \ell_{1,m+1} & \ell_{2,m+1} & \dots & \ell_{m,m+1} \\ \ell_{1,m+2} & \ell_{2,m+2} & \dots & \ell_{m,m+2} \\ \vdots & \vdots & \dots & \vdots \\ \ell_{1,n} & \ell_{2,n} & \dots & \ell_{m,n} \end{pmatrix} \quad (42)$$

and we recall that $\ell_{i,j}$ is the Gauss linking number between L_i and L_j , modulo k . As before, the matrix \mathbf{G} is interpreted as a map $\mathbf{G} : \mathbb{Z}_k^m \rightarrow \mathbb{Z}_k^{n-m}$, and so $|\ker \mathbf{G}|$ is defined as the number of solutions $\vec{x} \in \mathbb{Z}_k^m$ (once again, including the zero solution) to the system of congruences

$$\mathbf{G} \cdot \vec{x} = 0 \pmod{k}, \quad (43)$$

which can equivalently be written in terms of Diophantine equations if we so prefer. Once again the Renyi entropies are \mathbf{n} -independent. So we finally arrive at the entanglement entropy (i.e., the $\mathbf{n} \rightarrow 1$ limit of the Renyi entropy) for a generic n -component link bi-partitioned into an m -component link and its complement:

$$S_{EE;m|n-m}(\mathcal{L}^n) = \ln \left(\frac{k^m}{|\ker \mathbf{G}|} \right). \quad (44)$$

When $m = 1$, it is easy to show that³

$$|\ker \mathbf{G}| = \gcd(k, \ell_{12}, \ell_{13}, \dots, \ell_{1n}), \quad (45)$$

and consequently we have a completely explicit formula for the entanglement entropy. For $m > 1$, we do not know of such an explicit formula for $|\ker \mathbf{G}|$. Nevertheless, as a demonstration of the usefulness of equation (44) we can compute an interesting information theoretic quantity called the *tri-partite mutual information*:

$$I_3(L_1, L_2, L_3) = I(L_1, L_2) + I(L_1, L_3) - I(L_1, L_2 \cup L_3) \quad (46)$$

in, for instance, a four-component simple chain, for which $\ell_{12} = \ell_{23} = \ell_{34} = 1$ while the rest of the linking numbers vanish. A direct computation shows that in this case

$$I_3 = -\ln k < 0 \quad (47)$$

thus indicating genuine tri-partite entanglement in this state. However, the mutual information in these link states does not satisfy monogamy, namely it is possible to construct explicit examples where $I_3 > 0$. For instance, this is the case if we take $\ell_{i,j} = 1$ for all $i \neq j$, in which case one finds $I_3 = \ln k$. A more complete investigation of multi-partite entanglement and the entropy cone in this system will be left to future work.

We are now in a position to answer the following question: what type of topology in a link is detected by the Abelian entanglement entropy? It is clear from the definition (42), that if the Gauss linking matrix \mathbf{G} vanishes (i.e., $\mathbf{G} = 0 \pmod{k}$), then $|\ker \mathbf{G}| = k^m$. Consequently, the above expression for $S_{EE;m|n-m}$ implies that the entanglement entropy vanishes. Conversely, if the entropy

³We can use $S_{EE}(A) = S_{EE}(A^c)$ to obtain $|\ker \mathbf{G}^T| = k^{n-2m} |\ker \mathbf{G}|$. For $m = 1$, this gives a very simple proof that the number of solutions to the congruence $a_1 x_1 + \dots + a_{n-1} x_{n-1} = 0 \pmod{k}$ is equal to $k^{n-2} \gcd(k, a_1, a_2, \dots, a_{n-1})$, a result found in standard number theory texts [22].

$S_{EE;m|n-m}$ vanishes, then this implies that $|\ker \mathbf{G}| = k^m$. In other words, every point in \mathbb{Z}_k^m lies in the kernel of \mathbf{G} . By applying this condition to special points like $(1, 0, 0, \dots, 0)$, $(0, 1, 0, \dots, 0)$ etc., we then learn that all the elements of \mathbf{G} are $0 \pmod k$. Hence, the linking matrix vanishes, modulo k . Therefore, we have proven that *the quantum entanglement entropy in $U(1)_k$ Chern-Simons theory for an $(m|n-m)$ bi-partition of a generic n -component link vanishes if and only if the corresponding linking matrix \mathbf{G} vanishes (modulo k)*. In this sense, the entanglement entropy in $U(1)_k$ Chern-Simons theory detects Gauss linking modulo k .

4 Non-Abelian case: $G = SU(2)_k$

In this section, we will compute the multi-boundary entanglement entropies in the case of a non-Abelian group, $SU(2)_k$. In contrast to the $U(1)_k$ case, the calculation of the entropies cannot be carried out in complete generality. So our strategy will be to work out the entropies for several interesting cases of two- and three-component links, and will then discuss general lessons from these examples.

4.1 Two-component states

The simplest non-trivial two-component link is the Hopf link (Figure 5), denoted by 2_1^2 in Rolfsen notation. It is possible to evaluate the entanglement entropy in the corresponding state $|2_1^2\rangle$ in

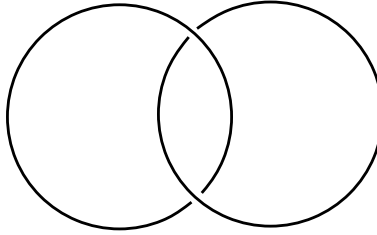


Figure 5: The Hopf-link.

several different ways. In fact, the coloured link invariants that define the wavefunction, $C_{2_1^2}(j_1, j_2)$, are given by the modular \mathcal{S} -matrix elements [12]

$$C_{2_1^2}(j_1, j_2) = \mathcal{S}_{j_1 j_2}, \quad (48)$$

where recall that \mathcal{S} implements the global diffeomorphism $\tau \rightarrow -\frac{1}{\tau}$ on the torus, and for $SU(2)_k$ is explicitly given by

$$\mathcal{S}_{j_1 j_2} = \sqrt{\frac{2}{k+2}} \sin \left(\frac{(2j_1+1)(2j_2+1)\pi}{k+2} \right) \quad (49)$$

The only property of \mathcal{S} which is relevant presently is that it is unitary. Using this property, it is a simple exercise to show that the normalized reduced density matrix after tracing out the first link is given by

$$\rho_2(2_1^2) = \frac{1}{\langle 2_1^2 | 2_1^2 \rangle} \text{Tr}_{L_1} |2_1^2\rangle \langle 2_1^2| = \frac{1}{\dim(\mathcal{H}(T^2))} \sum_j |j\rangle \langle j| \quad (50)$$

Consequently, one finds the entanglement entropy

$$S_{EE}(2_1^2) = \ln \dim(\mathcal{H}(T^2)) = \ln(k+1) \quad (51)$$

which implies that the Hopf link state is maximally entangled. *In other words, the Hopf link is analogous to a Bell pair in quantum information theory.* We encountered this fact in the $U(1)_k$ case as well. The same result can also be obtained using the replica trick. The link complement corresponding to the Hopf link is $T^2 \times I$, where I is an interval. Hence, replicating the manifold makes a longer interval, and taking the trace turns the interval into a circle. Thus, the Renyi entropy essentially amounts to computing the log of the partition function over $S^1 \times T^2$; a direct computation then yields the above result.

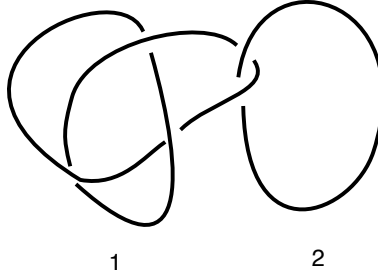


Figure 6: A link between a trefoil knot and an unknot, i.e., the connected sum of the trefoil knot with the Hopf link.

Having studied the Hopf link, it is natural to ask what happens if we replace the individual unknots inside the Hopf link with more complicated knots. In other words, given two knots K_1 and K_2 , what is the link state corresponding to “Hopf-linking” these two knots together? (see for instance Figure 6 which illustrates this link for the case of K_1 being a trefoil and K_2 being an unknot). More precisely, we are asking for the link state corresponding to the *connected sum* $K_1 + 2_1^2 + K_2$ (see [12] for further details).⁴ It is a simple matter (again following [12]) to write down the state corresponding to this connected sum:

$$|K_1 + 2_1^2 + K_2\rangle = \sum_{j_1, j_2} \frac{C_{K_1}(j_1)}{\mathcal{S}_{0j_1}} \mathcal{S}_{j_1 j_2} \frac{C_{K_2}(j_2)}{\mathcal{S}_{0j_2}} |j_1, j_2\rangle \quad (52)$$

For simplicity, let us pick K_2 to be the unknot. The normalized reduced density matrix over the

⁴Such a connected sum is not unique in general, but does not apply in the case we’re studying.

first component then takes the form

$$\rho_1(K_1 + 2_1^2 + K_2) = \sum_j p_j |j\rangle\langle j|, \quad p_j = \frac{|\frac{C_{K_1}(j)}{S_{0j}}|^2}{\sum_{j'} |\frac{C_{K_1}(j')}{S_{0j'}}|^2} \quad (53)$$

and therefore the entanglement entropy in this case is given by

$$S_{EE}(K_1 + 2_1^2 + K_2) = - \sum_j p_j \ln p_j. \quad (54)$$

Indeed, if we take K_1 to be the unknot as well, then we recover the earlier result for the Hopf link. But in general if K_1 is some non-trivial knot, then the entropy of entanglement is smaller. This demonstrates that *the non-Abelian entanglement entropy detects knotting of the individual components inside a link, something to which the Abelian theory was insensitive.*

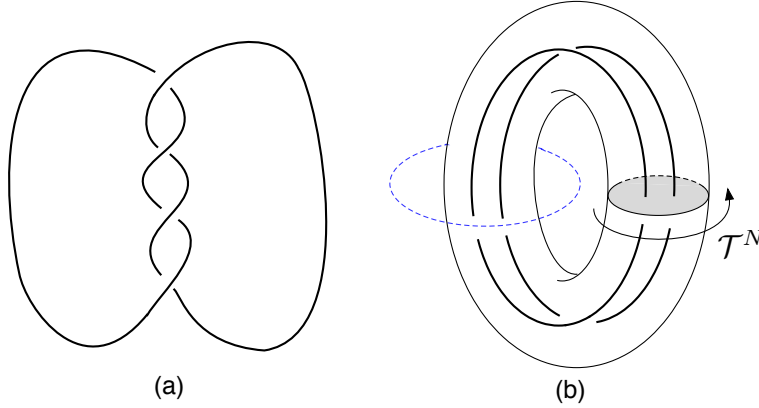


Figure 7: (a) The two component link 4_1^2 . This is a special case of the family of links $2N_1^2$ with $N = 2$. (b) One way to evaluate the corresponding link invariant for general N is to perform surgery along the dashed blue circle. The twisting of the link is accomplished by using a Dehn twist \mathcal{T}^N as indicated.

To gain further practice, let us study some additional two-component links. We start with 4_1^2 (see Figure 7), which is similar to the Hopf link, but with two twists (or four crossings). In fact, we can instead study the generalization of 4_1^2 to $2N$ crossings, which we will here denote by $2N_1^2$ (although this is perhaps not the standard terminology). We can explicitly evaluate this state. To do so, we picture two unlinked circles inside a solid torus and then perform an N -fold Dehn-twist on the torus to link the circles together. Finally, we perform a modular \mathcal{S} transform and glue the result with an empty solid torus (see Figure 7 (b) for a pictorial explanation of how this is done and [12] for the details of the general procedure of surgery). This gives

$$|2N_1^2\rangle = \sum_{j_1, j_2} \sum_m (\mathcal{S}\mathcal{T}^N\mathcal{S})_{0m} \frac{\mathcal{S}_{j_1 m} \mathcal{S}_{j_2 m}}{\mathcal{S}_{0m}} |j_1, j_2\rangle \quad (55)$$

where we recall that \mathcal{T} acts by a phase in our basis $\mathcal{T}|m\rangle = e^{2\pi i h_m} |m\rangle$. The entanglement entropy

is therefore given by

$$S_{EE} = - \sum_m p_m \ln p_m, \quad p_m = \frac{\left| \frac{(\mathcal{ST}^N \mathcal{S})_{0m}}{\mathcal{S}_{0m}} \right|^2}{\sum_n \left| \frac{(\mathcal{ST}^N \mathcal{S})_{0n}}{\mathcal{S}_{0n}} \right|^2} \quad (56)$$

Since the case $N = 1$ (i.e., the Hopf link) is maximally entangled, the entanglement entropy for higher N will generically be smaller (or equal) to the entropy of the Hopf link (see Figure 8).⁵

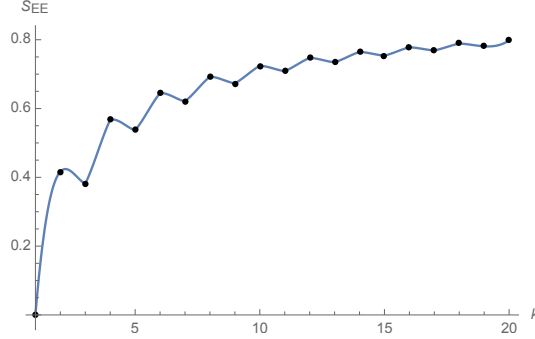


Figure 8: The entanglement entropy of 4_1^2 as a function of k . The blue line is an interpolating curve.

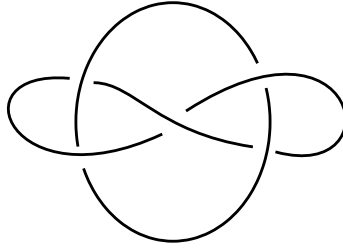


Figure 9: The Whitehead link.

Finally, the last two-component link we will study here is 5_1^2 , also called the Whitehead link (Figure 9). The Gauss linking number vanishes in this case, but the link is nevertheless topologically non-trivial. The coloured link invariant for the Whitehead link can be computed using a remarkable formula due to K. Habiro [23–25]:

$$C_{5_1^2}(j_1, j_2) = \sum_{i=0}^{\min(j_1, j_2)} q^{-\frac{i(i+3)}{4}} (q^{1/2} - q^{-1/2})^{3i} \frac{[2j_1 + i + 1]! [2j_2 + i + 1]! [i]!}{[2j_1 - i]! [2j_2 - i]! [2i + 1]!} \quad (57)$$

where

$$[x] = \frac{q^{x/2} - q^{-x/2}}{q^{1/2} - q^{-1/2}}, \quad [x]! = [x][x-1] \cdots [1], \quad q = e^{\frac{2\pi i}{k+2}}. \quad (58)$$

⁵This might seem somewhat counter-intuitive; one might naively have expected that the $N > 1$ links are even more entangled. However, it is easy to trace this decrease in entanglement entropy to an increase in the *relative entropy* between the reduced density matrix for $2N_1^2$ and 2_1^2 . Since the Hopf link was maximally entangled, the only way for this relative entropy to increase is for the $N > 1$ links to be less entangled.

The result for the entanglement entropy is shown in Figure 10. The fact that the Whitehead link has non-trivial entanglement entropy again confirms that *the non-Abelian entropy is sensitive not merely to Gauss linking, but to more intricate forms of topological entanglement*.

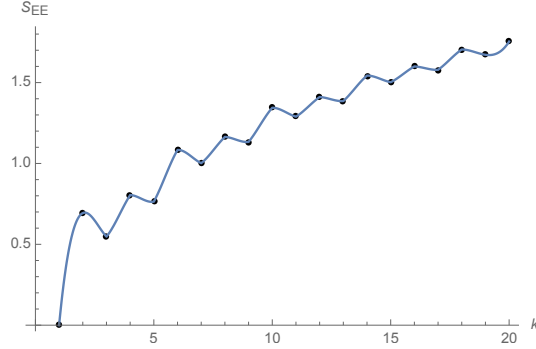


Figure 10: The entanglement entropy for the Whitehead link as a function of k . The blue line is an interpolating curve.

There is also a second way to compute the coloured link invariant for the Whitehead link using monodromy properties of conformal blocks of the chiral $SU(2)_k$ WZW model. This method has been explained in detail in [26–28] and will be reviewed in Appendix A. We merely quote the result here:

$$\begin{aligned}
C_{5_1^2}(j_1, j_2) &= [2j_1 + 1]^2 [2j_2 + 1] \sum_{\mathbf{m}, \mathbf{n}, \mathbf{p}} \lambda_{p_1, -}^{-1}(j_1, j_2) \lambda_{p_2, +}(j_1, j_2) \lambda_{n_1, +}^{-1}(j_1, j_2) \lambda_{m_1, -}^{-1}(j_1, j_2) \lambda_{m_2, +}(j_1, j_2) \\
&\times a_{(\mathbf{0}, \mathbf{p})} \begin{pmatrix} j_1 & j_1 \\ j_2 & j_2 \\ j_1 & j_1 \end{pmatrix} a_{(\mathbf{n}, \mathbf{p})} \begin{pmatrix} j_1 & j_2 \\ j_1 & j_1 \\ j_2 & j_1 \end{pmatrix} a_{(\mathbf{n}, \mathbf{m})} \begin{pmatrix} j_1 & j_2 \\ j_1 & j_1 \\ j_2 & j_1 \end{pmatrix} a_{(\mathbf{0}, \mathbf{m})} \begin{pmatrix} j_1 & j_1 \\ j_2 & j_2 \\ j_1 & j_1 \end{pmatrix}. \quad (59)
\end{aligned}$$

where the $a_{(\mathbf{n}, \mathbf{p})}$'s are duality transformations acting on 6-point conformal blocks on S^2 , and the λ 's are phases which these blocks pick up under the action of braid generators. In Appendix A all the quantities appearing in equation (59) are explained in detail. The relevant point here is that there exists an algorithmic way to compute coloured link invariants using conformal blocks for the Whitehead link, and indeed more generally for arbitrary links. We have also computed the entanglement entropy for the Whitehead link using this second approach for small values of k , and we find precise agreement with the results obtained from the Habiro formula.

4.2 Three-component states

We now consider a few examples of three-component links and discuss their entanglement structure. Let us begin by considering the link in Figure 11. This link is a connected sum of two Hopf links.

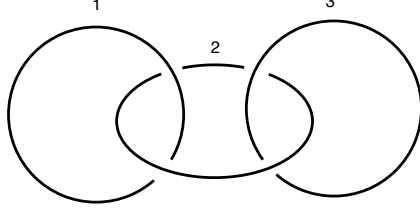


Figure 11: A three component link which is the connected sum of two Hopf links.

Consequently, we can evaluate the link invariant explicitly following [12], and we find that the corresponding link state is given by

$$|2_1^2 + 2_1^2\rangle = \sum_{j_1, j_2, j_3, m} \mathcal{S}_{j_2 m} N_{m j_1 j_3} |j_1, j_2, j_3\rangle = \sum_{j_1, j_2, j_3} \frac{\mathcal{S}_{j_1 j_2} \mathcal{S}_{j_3 j_2}}{\mathcal{S}_{0 j_2}} |j_1, j_2, j_3\rangle \quad (60)$$

where N_{ijm} is the *fusion coefficient*, namely the dimension of the Hilbert space on S^2 with Wilson lines in the representations i, j, m piercing through, or equivalently the number of times the representation m appears in the product of the representations i and k .⁶ We have also used the Verlinde formula [29]

$$N_{ikm} = \sum_j \frac{\mathcal{S}_{ij} \mathcal{S}_{kj} \mathcal{S}_{mj}}{\mathcal{S}_{0j}}. \quad (61)$$

So we can compute the entanglement entropies for this state explicitly⁷, and we find (Figure 12)

$$S_{EE; (L_2 | L_1, L_3)}(2_1^2 + 2_1^2) = S_{EE; (L_1 | L_2, L_3)}(2_1^2 + 2_1^2) = - \sum_i p_i \ln p_i, \quad p_i = \frac{d_i^{-2}}{\sum_j d_j^{-2}} \quad (62)$$

where $d_j = [2j + 1] = \frac{\mathcal{S}_{0j}}{\mathcal{S}_{00}}$ is the quantum dimension of the representation j . Interestingly, the

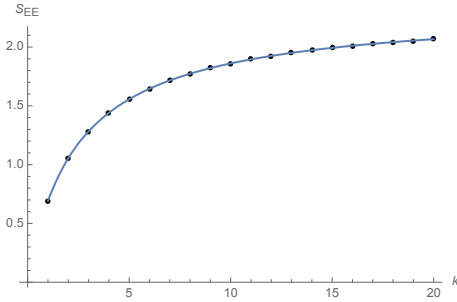


Figure 12: The entanglement entropy $S_{EE; L_2 | L_1, L_3}$ for the connected sum of two Hopf links as a function of k .

entropy is independent of which link we trace out. Furthermore, tracing out any of the links leaves

⁶Another equivalent way to specify the fusion coefficients is to specify the fusion algebra, which for $SU(2)_k$ is given by:

$$j_1 \otimes j_2 = |j_1 - j_2|, |j_1 - j_2| + 1, \dots, \min(j_1 + j_2, k - j_1 - j_2).$$

⁷This can be done by changing bases on L_1 and L_3 to $|\hat{j}\rangle = \sum_{j'} \mathcal{S}_{jj'} |j'\rangle$.

us with a *separable* reduced density matrix on the other two links, as can be checked explicitly. In this sense, the above link state has “GHZ-like” entanglement. These properties might sound puzzling at first. Indeed, the above discussion makes it clear that the entanglement entropy (and in fact the entanglement spectrum) in this case contains fairly coarse information, and is insufficient to distinguish between the topological linking between for instance the subcomponents 1 and 2 or 1 and 3. Of course, the quantum state has much more fine-grained information which can be potentially extracted by using other probes. For instance, here is one simple-minded way of doing this — let us define the projector

$$\mathbf{P}(L_\alpha) = |0\rangle\langle 0|_{L_\alpha} \quad (63)$$

which projects the state on L_α to the spin-0 state $|0\rangle$. We can use $\mathbf{P}(L_\alpha)$ to further probe the entanglement structure of the state $|2_1^2 + 2_1^2\rangle$. Acting on various factors of the state (60) with the projector, we get

$$\mathbf{P}(L_1)|2_1^2 + 2_1^2\rangle = \sum_{j_1, j_2} \mathcal{S}_{j_1 j_2} |0\rangle \otimes |j_1, j_2\rangle \quad (64)$$

$$\mathbf{P}(L_2)|2_1^2 + 2_1^2\rangle = \sum_{j_1, j_1} \frac{\mathcal{S}_{j_1 0} \mathcal{S}_{j_2 0}}{\mathcal{S}_{00}} |j_1\rangle \otimes |0\rangle \otimes |j_2\rangle \quad (65)$$

Note that the latter state is simply a product state. This is easy to understand from the topological structure of the link – the projector $\mathbf{P}(L_2)$ essentially erases the second link (that is, a Wilson loop in the spin-0 state is trivial), due to which the link in Figure 11 entirely falls apart into an unlink. So

$$S_{EE, L_1 | L_3}(\mathbf{P}(L_2)|2_1^2 + 2_1^2\rangle) = 0 \quad (66)$$

where we are computing the entanglement entropy of the (pure) state on the links left untouched by the projector. On the other hand, projecting on L_1 erases this subcomponent, but the state on the other two links is still non-trivially entangled, mirroring the topological linking in Figure 11. Indeed, in this case, we find

$$S_{EE, L_2 | L_3}(\mathbf{P}(L_1)|2_1^2 + 2_1^2\rangle) = \ln(k+1) \quad (67)$$

So the above *projected* entanglement entropies give additional information theoretic measures to probe topological entanglement of links. However, we should emphasize here that we have chosen to project in a particular basis which is natural to the problem; the corresponding entropies are therefore basis-dependent quantities.

A basis independent entropic measure that probes how multicomponent links are knotted is the *relative entropy* of the state after being reduced on different links. Recall that for two states ρ and σ , the relative entropy is defined by

$$S(\rho || \sigma) = \text{Tr}(\rho \ln \rho) - \text{Tr}(\rho \ln \sigma) \quad (68)$$

For a three component state ρ , computing $S(\rho_{L_1} || \rho_{L_2})$ gives a basis independent measure of the distinguishability of ρ reduced on link L_1 (i.e. where we trace out L_2 and L_3) against ρ reduced on L_2 (i.e. where we trace out L_1 and L_3). For instance, considering the chain state (connected sum of Hopf links) $|2_1^2 + 2_1^2\rangle$, the entanglement spectrum of $\rho_{L_1}(2_1^2 + 2_1^2)$ is the same as ρ_{L_2} ; however the bases that diagonalize these matrices are different. Therefore we expect the relative entropy between these two reduced states to be nonzero and indeed we find⁸

$$S(\rho_{L_1}(2_1^2 + 2_1^2) || \rho_{L_2}(2_1^2 + 2_1^2)) = \sum_i p_i \left(\ln p_i - \sum_j |\mathcal{S}_{ij}|^2 \ln p_j \right) \quad (69)$$

with p_j being given by (62). While the projected entropy has the interpretation of erasing a link, it is not clear that the relative entropy between reduced states has a nice pictorial interpretation. However, we see that it is a useful entropic measure of the distinguishability of individual components within a given link.

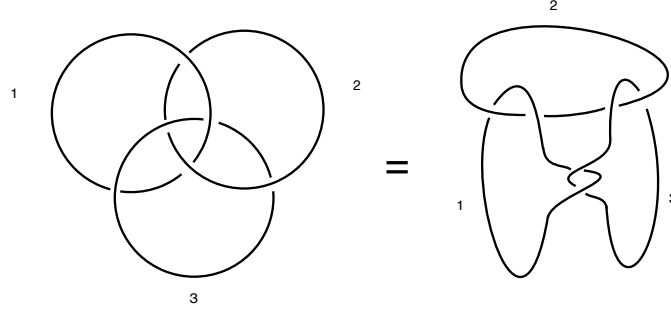


Figure 13: The three component link 6_3^3 .

Let us now consider a slightly more complicated three-component link called 6_3^3 , which is shown in Figure 13. This differs from the connected sum state we considered previously by a Dehn-twist on a torus surrounding the links 1 and 3. So we can write this state explicitly as well:

$$\begin{aligned} |6_3^3\rangle &= \sum_{j_1, j_2, j_3, m} e^{2\pi i(h_m - h_{j_1} - h_{j_3})} \mathcal{S}_{mj_2} N_{mj_1 j_3} |j_1, j_2, j_3\rangle \\ &= \sum_{j_1, j_2, j_3} \sum_{m, n} e^{2\pi i(h_m - h_{j_1} - h_{j_3})} \frac{\mathcal{S}_{mj_2} \mathcal{S}_{j_1 n} \mathcal{S}_{j_3 n} \mathcal{S}_{mn}}{\mathcal{S}_{0n}} |j_1, j_2, j_3\rangle \end{aligned} \quad (70)$$

where we have used the fact that the Dehn twist acts by a phase in our basis $\mathcal{T}|m\rangle = e^{2\pi i h_m} |m\rangle$ ⁹. We can simplify the above expressions by using the property $(\mathcal{ST})^3 = 1$ (see Section 2), which leads us to

$$|6_3^3\rangle = \sum_{j_1, j_2, j_3} \sum_n e^{-2\pi i(h_n + h_{j_1} + h_{j_2} + h_{j_3})} \frac{\mathcal{S}_{j_1 n} \mathcal{S}_{j_2 n} \mathcal{S}_{j_3 n}}{\mathcal{S}_{0n}} |j_1, j_2, j_3\rangle. \quad (71)$$

⁸This calculation, along with other various relative entropies can be found in Appendix B.

⁹We have also corrected for a change in framing that results from the action of \mathcal{T} , although this is not strictly required for our purposes.

Interestingly, the entanglement entropies corresponding to this state are precisely equal to the entanglement entropies for the chain of Hopf links $2_1^2 + 2_1^2$:

$$S_{EE; L_2|L_1, L_3}(6_3^3) = S_{EE; L_1|L_2, L_3}(6_3^3) = S_{EE; L_3|L_1, L_2}(6_3^3) = - \sum_i p_i \ln p_i, \quad p_i = \frac{d_i^{-2}}{\sum_j d_j^{-2}} \quad (72)$$

Additionally, tracing out any of the links in this state once again leads to a *separable* reduced density matrix on the other two links. This once again implies that this state, like $2_1^2 + 2_1^2$ has “GHZ-like” entanglement (by which we mean that the reduced density matrix obtained by tracing out one of the tori is separable). However, we can distinguish it from the chain of Hopf links state by looking at the projected entropies, namely the entropies after the action of the projector \mathbf{P} . Indeed, it is clear from equation (71) that all the projected entropies for 6_3^3 are equal and are given by

$$S_{EE, L_2|L_3}(\mathbf{P}(L_1)|6_3^3) = S_{EE, L_1|L_3}(\mathbf{P}(L_2)|6_3^3) = S_{EE, L_1|L_2}(\mathbf{P}(L_3)|6_3^3) = \ln(k+1). \quad (73)$$

Notably, the projected entropies for 6_3^3 are very different from the projected entropies for $2_1^2 + 2_1^2$, and indeed mirror the topological linking structure of the respective links. Similarly, a short calculation of the relative entropy between the reduced 6_3^3 state and the reduced $2_1^2 + 2_1^2$ state distinguishes these links. For instance, reducing each link on its second component (i.e. tracing out L_1 and L_3), we have

$$S(\rho_{L_2}(6_3^3) || \rho_{L_2}(2_1^2 + 2_1^2)) = \sum_i p_i \left(\ln p_i - \sum_j |\mathcal{S}_{ij}|^2 \ln p_j \right). \quad (74)$$

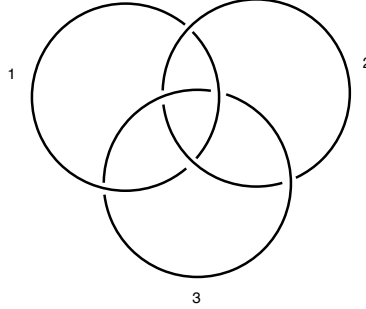


Figure 14: Borromean rings.

Finally, we compute the entanglement entropy for the Borromean rings 6_2^3 (see Figure 14). In this case, the coloured link invariants can once again be computed by using Habiro’s formula [23, 24],¹⁰ which in this case reads:

$$C_{6_2^3}(j_1, j_2, j_3) = \sum_{i=0}^{\min(j_1, j_2, j_3)} (-1)^i (q^{1/2} - q^{-1/2})^{4i} \frac{[2j_1 + i + 1]! [2j_2 + i + 1]! [2j_3 + i + 1]! ([i]!)^2}{[2j_1 - i]! [2j_2 - i]! [2j_3 - i]! ([2i + 1]!)^2} \quad (75)$$

¹⁰This formula can be checked explicitly (at least for small values of k) using the monodromy of conformal blocks method which is discussed in Appendix A. We find precise agreement in the cases we have checked.

in the notation introduced in equation (58). Using this formula, it is possible to compute the entanglement entropies for this link as a function of k , and the result is shown in Figure 15. Once

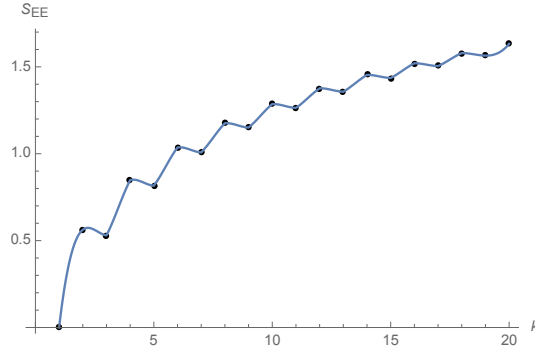


Figure 15: The entanglement entropy for the Borromean rings as a function of k .

again, we find that the entropy is non-vanishing in this case. The Borromean rings have trivial Gauss linking between any two circles. Further, they have the special property that if we erase any circle from the link, the remaining two circles become unlinked; such links are called *Brunnian* links. This latter property can be cast in terms of the projected entropies as the statement that

$$S_{EE,L_2|L_3}(\mathbf{P}(L_1)|6_2^3\rangle) = S_{EE,L_1|L_3}(\mathbf{P}(L_2)|6_2^3\rangle) = S_{EE,L_1|L_2}(\mathbf{P}(L_3)|6_2^3\rangle) = 0. \quad (76)$$

Finally, the reduced density matrix for the Borromean rings upon tracing out one of the links (say L_3) is *not* separable. The easiest way to see this in the present case is to compute the *entanglement negativity* [30, 31] (see also [32]), which is defined as follows. For a given (possibly mixed) density matrix ρ on a bi-partite system (in the present case on $L_1 \cup L_2$), let us start by defining the partial transpose ρ^Γ :

$$\langle j_1, j_2 | \rho^\Gamma | \tilde{j}_1, \tilde{j}_2 \rangle = \langle j_1, \tilde{j}_2 | \rho | \tilde{j}_1, j_2 \rangle. \quad (77)$$

Then, the number of negative eigenvalues of ρ^Γ is known to be a good measure of quantum entanglement. A good quantitative way to capture this is the entanglement negativity, which is defined as¹¹

$$\mathcal{N} = \frac{\|\rho^\Gamma\| - 1}{2}. \quad (78)$$

More importantly for us, a non-zero value of \mathcal{N} (i.e., $\mathcal{N} > 0$) necessarily implies that the reduced density matrix is not separable. The negativity for the reduced density matrix on $L_1 \cup L_2$ for the Borromean rings is shown in Figure 16. We find that $\mathcal{N} > 0$ for $k > 1$, thus showing that the Borromean rings have a more robust, “W-like” entanglement structure (by which we mean that the reduced density matrix obtained by tracing out one of the tori is not separable).

¹¹The trace norm is defined as $\|O\| = \text{Tr}(\sqrt{O^\dagger O})$.

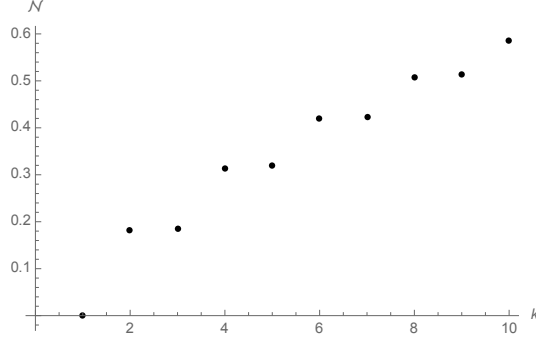


Figure 16: The entanglement negativity between links L_1 and L_2 upon tracing out L_3 for the Borromean rings as a function of k .

5 Discussion

To conclude, we have studied multi-boundary entanglement in Chern-Simons theory for states defined on n copies of a torus T^2 . We have focussed on the specific class of states prepared by performing the path-integral of Chern-Simons theory on link complements of n -component links in S^3 . For $U(1)_k$ Chern-Simons theory, we gave a general formula for the entanglement entropy of a generic bi-partition of the link into two sub-links. This formula involves the number of solutions of certain congruences (or equivalently Diophantine equations) with coefficients closely related to the Gauss-linking numbers between the two sub-links, and as such relates simple but interesting concepts from quantum information theory, knot theory and number theory. In the non-Abelian $SU(2)_k$ case, we studied the entanglement structure of several two- and three-component links. In particular, we showed that the Hopf link is maximally entangled and thus analogous to a Bell-pair from quantum information theory. We found examples of three component links – such as 6^3_3 – with “GHZ-like” entanglement (namely that they have non-trivial, but not necessarily maximal¹² entanglement entropies under bi-partitions, but they reduce to separable states upon tracing out one of the links). Finally, we showed that the Borromean rings have a more robust “W-like” entanglement structure, namely that they have non-trivial (again, not necessarily maximal) entanglement under bi-partitions, and in addition the reduced density matrix upon tracing out one of the links is not separable. We end with some open questions.

Generally speaking, a main message of this paper is that quantum information theoretic ideas applied to multi-boundary states in Chern-Simons theory can provide interesting, and potentially powerful tools in the study of knot theory. In this direction, we studied only simple quantities such as entanglement entropies, Renyi entropies, etc., which turn out to be sums over quantities involving the coloured link invariants. Said another way, the entanglement entropies extract certain

¹²Although note that in $U(1)_k$, the 6^3_3 link additionally also has maximal entanglement under bi-partitions.

coarse-grained framing independent information from the coloured link invariants. In the $U(1)_k$ theory, we showed that these entropies are powerful enough to detect Gauss linking (mod k), namely that the entanglement entropy for a bi-partition vanishes if and only if the Gauss linking matrix between the two sub-links vanishes (mod k). In the non-Abelian case, the corresponding statement remains unclear — it is clear that quantum entanglement implies topological linking, but the converse remains to be shown. In other words, does there exist a link where the coloured link invariants all factorize along a bi-partition, despite non-trivial topological linking between the corresponding sublinks? This is of course also related to a famous question — do any coloured link invariants detect the unlink? In this context, there are known examples of non-trivial links which the Jones polynomial does not distinguish from the unlink [33]. It will be interesting to compute the entanglement entropies in these examples. Additionally, it will be of interest to generalize these results to other gauge groups, such as $SU(N)$.

The discussion above mostly focussed on using quantum information theory to study links. In the opposite direction, we can ask whether knot theory can shed light on unsolved problems in quantum information theory. It is an old idea that quantum entanglement might be interpreted in terms of topological entanglement in links (see for instance [34–37] and references therein). We have argued in this paper that multi-boundary states in Chern-Simons theory provide the right framework for realizing this idea. It would be interesting to study whether this connection between quantum entanglement and topological linking can be used effectively in better understanding multi-partite entanglement structures. A first exercise in this direction would be to characterize the entropy cone for multi-boundary states, perhaps in the simpler set-up of $U(1)_k$ Chern Simons theory. It would also be very useful to study the entanglement structure of four and higher component links in the non-Abelian case.

Finally, it would be interesting to study multi-boundary entanglement in $SL(2, \mathbb{C})$ Chern-Simons theory, which is closely related with quantum gravity in three dimensions. One might expect the multi-boundary entanglement entropy in this context to admit a *geometric* description, beyond topology. In fact, it is known that many links (and knots) admit a geodesically complete hyperbolic metric on their link-complements – such links are called hyperbolic links. For such links, it is conjectured that the logarithm of the reduced $SU(2)$ coloured link invariant with each component carrying the N dimensional representation, evaluated at $q = e^{2\pi i/N}$, asymptotes in the $N \rightarrow \infty$ limit to the volume of the hyperbolic metric, a statement which is called the *volume conjecture* [38–40]. Along similar lines, it would be interesting to explore whether the entropies we have defined and computed in this paper also admit a geometric description in terms of the hyperbolic metric on the link complement. Indeed, it would not be unreasonable to hope that the entropy corresponds to the area of some minimal surface (or a horizon in the Lorentzian continuation) in the $k \rightarrow \infty$ limit.

Of course, this remark is motivated by the Bekenstein-Hawking formula for black-hole entropy, and the Ryu-Takayanagi formula for entanglement entropy in the AdS/CFT correspondence.

Note Added: After this work was completed, we were made aware of the recent work of Salton, Swingle and Walter [41], which has some overlap with our work. These authors investigate how different states can be prepared on a union of tori in Chern-Simons theory by considering different 3-manifolds with the same boundary. Their main result is that the states constructed this way in $U(1)_k$ Chern-Simons theory can be interpreted as stabilizer states; this is consistent with the fact that the Abelian Renyi entropies computed in this paper are all equal. They also show that any state in $SO(3)$ Chern-Simons theory can be approximated arbitrarily well through a Euclidean path integral.

6 Acknowledgments

We gratefully acknowledge helpful conversations with Matt DeCross, Tom Faulkner, Arjun Kar, Valentijn Karemaker, Sheldon Katz, Romesh Kaul, Christopher Leininger, Aitor Lewkowycz, Alex Maloney, Henry Maxfield, Djordje Minic, Charles Rabideau, Srinidhi Ramamurthy, Grant Salton, Gabor Sarosi, Brian Swingle, Apoorv Tiwari, Mark Van Raamsdonk and Beni Yoshida. Research supported in part by the U.S. Department of Energy under contracts DE-SC0015655 and DE-FG02-05ER-41367, and by the Simons Foundation (#385592, Vijay Balasubramanian) through the It From Qubit Simons Collaboration. V.B. and O.P. also thank the Perimeter Institute for hospitality during the It From Qubit workshop and school.

A Link invariants from monodromies of conformal blocks

In this appendix, we review the calculation of coloured link invariants from the monodromy properties of conformal blocks of the $SU(2)_k$ chiral WZW model. We will only review here the recipe for these computations, following [26–28] (see [42] for requisite background material); we refer the reader to these papers for further details. Since these techniques are required in this paper for the two special cases of the Whitehead link and the Borromean rings, we will present our discussion in the context of these examples, but the techniques straightforwardly generalize to other links.

A.1 Whitehead link

Our basic ingredients in constructing link invariants will be S^2 conformal blocks of chiral vertex operators in $SU(2)_k$ WZW theory. For the case of the Whitehead link (and also Borromean rings), we need the six-point blocks $\phi_{\mathbf{p}}$ and $\phi'_{\mathbf{q}}$ shown in Figure 17 below. The two different fusion channels correspond to two different choices of a basis for the Hilbert space of Chern-Simons theory with six Wilson lines piercing through the 2-sphere. In fact, both $\phi_{\mathbf{p}}$ and $\phi'_{\mathbf{q}}$ are orthonormal bases for the space of six-point conformal blocks on S^2 (see Figure 17), and as such are related by a duality transformation $a_{(\mathbf{p},\mathbf{q})}$:

$$|\phi_{\mathbf{p}}(j_1, j_2, \dots, j_6)\rangle = \sum_{\mathbf{q}} a_{(\mathbf{p},\mathbf{q})} \begin{pmatrix} j_1 & j_2 \\ j_3 & j_4 \\ j_5 & j_6 \end{pmatrix} |\phi'_{\mathbf{q}}(j_1, j_2, \dots, j_6)\rangle \quad (79)$$

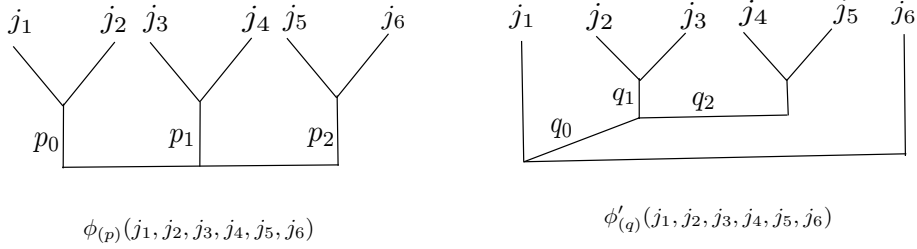


Figure 17: Two different basis for 6-point conformal blocks.

The $a_{(\mathbf{p},\mathbf{q})}$ can also be written in terms of a sequence of four-point duality transformations:

$$a_{(\mathbf{p},\mathbf{q})} \begin{pmatrix} j_1 & j_2 \\ j_3 & j_4 \\ j_5 & j_6 \end{pmatrix} = \sum_t a_{t,p_1} \begin{pmatrix} p_0 & j_3 \\ j_4 & p_2 \end{pmatrix} a_{p_0,q_1} \begin{pmatrix} j_1 & j_2 \\ j_3 & t \end{pmatrix} a_{p_2,q_2} \begin{pmatrix} t & j_4 \\ j_5 & j_6 \end{pmatrix} a_{t,q_0} \begin{pmatrix} j_1 & q_1 \\ q_2 & j_6 \end{pmatrix} \quad (80)$$

where $a_{j,l}$ are the fusion matrices for four-point block and are given explicitly by:

$$\begin{aligned} a_{j,l} \begin{pmatrix} j_1 & j_2 \\ j_3 & j_4 \end{pmatrix} &= (-1)^{j_1+j_2-j_3-j_4-2j} \sqrt{[2j+1][2l+1]} \Delta(j_1, j_2, j) \Delta(j_3, j_4, j) \Delta(j_1, j_4, l) \Delta(j_2, j_3, l) \\ &\times \sum_{m \geq 0} (-1)^m [m+1]! \left\{ [m-j_1-j_2-j]! [m-j_3-j_4-j]! \right. \\ &\times [m-j_1-j_4-l]! [m-j_2-j_3-l]! [j_1+j_2+j_3+j_4-m]! \\ &\times [j_1+j_3+j+l-m]! [j_2+j_4+j+l-m]! \left. \right\}^{-1} \end{aligned} \quad (81)$$

where

$$\Delta(a, b, c) = \sqrt{\frac{[-a+b+c]! [-b+c+a]! [-c+a+b]!}{[a+b+c+1]!}} \quad (82)$$

and we have used the notation

$$[x] = \frac{q^{x/2} - q^{-x/2}}{q^{1/2} - q^{-1/2}}, \quad q = e^{\frac{2\pi i}{k+2}} \quad (83)$$

$$[x]! = [x][x-1][x-2] \cdots [1], \quad [0]! = 1 \quad (84)$$

Now coming to the Whitehead link, a plait representation of the link is shown in Figure 18. In

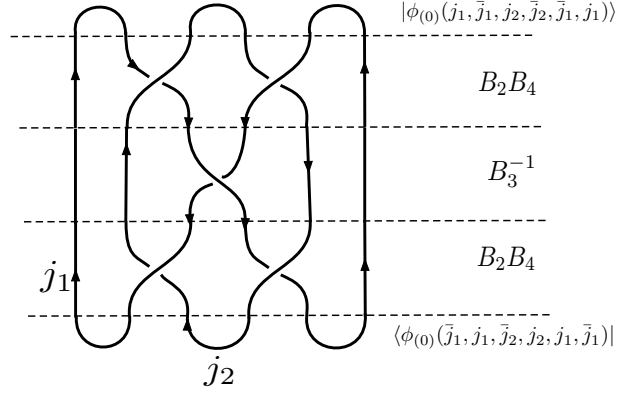


Figure 18: A plait representation of the Whitehead link 5_1^2 .

order to evaluate this link invariant, we imagine the plait representation as giving a transition amplitude between two states on S^2 with six operator insertions. As was argued in [27], the initial state (where by convention we take “time” to run from top to bottom) corresponds to the conformal block $\phi_{(0,0,0)}(j_1, \bar{j}_1, j_2, \bar{j}_2, \bar{j}_1, j_1)$, or more precisely

$$|\psi_i\rangle = [2j_1 + 1] \sqrt{[2j_2 + 1]} |\phi_{(0,0,0)}(j_1, \bar{j}_1, j_2, \bar{j}_2, \bar{j}_1, j_1)\rangle \quad (85)$$

while the final state similarly corresponds to the block $\phi_{(0,0,0)}(\bar{j}_1, j_1, \bar{j}_2, j_2, j_1, \bar{j}_1)$

$$|\psi_f\rangle = [2j_1 + 1] \sqrt{[2j_2 + 1]} |\phi_{(0,0,0)}(\bar{j}_1, j_1, \bar{j}_2, j_2, j_1, \bar{j}_1)\rangle \quad (86)$$

The operator insertions between the initial and final states implement the braiding of the various strands of the link. The operator B_{2m+1} generates a right handed braid between strand $2m + 1$ and $2m + 2$, while the operator B_{2m} generates a right-handed braid between the strand $2m$ and $2m + 1$. So we can write the Whitehead link invariant as

$$C_{5_1^2}(j_1, j_2) = \langle \psi_f | B_2 B_4 B_3^{-1} B_2 B_4 | \psi_i \rangle \quad (87)$$

In order to evaluate this amplitude, we need to use the fact that the blocks $|\phi_{(p_0, p_1, p_2)}(j_1, j_2, \dots, j_6)\rangle$ are eigenstates of odd numbered braiding operators

$$B_{2m+1} |\phi_{\mathbf{p}}(j_1, j_2, \dots, j_6)\rangle = \lambda_{p_m, \pm}^{\pm 1}(j_{2m+1}, j_{2m+2}) |\phi_{\mathbf{p}}(j_1, j_2, \dots, j_6)\rangle \quad (88)$$

where $\mathbf{p} = (p_0, p_1, p_2)$, and \pm stands for the relative orientation between the two strands which are being braided. The other set of blocks $\phi'_{\mathbf{q}}(j_1, j_2, \dots, j_6)$ on the other hand are eigenstates of the even braiding operators

$$B_{2m}|\phi'_{\mathbf{q}}(j_1, j_2, \dots, j_6)\rangle = \lambda_{q_m, \pm}^{\pm 1}(j_{2m+1}, j_{2m+2})|\phi'_{\mathbf{q}}(j_1, j_2, \dots, j_6)\rangle \quad (89)$$

The eigenvalues appearing above are precisely the monodromies of these conformal blocks, which are given by

$$\lambda_{t, \pm}(j_1, j_2) = (-1)^{j_1+j_2-t} q^{\pm \frac{C_{j_1}+C_{j_2}-C_t}{2}} \quad (90)$$

where $C_j = j(j+1)$, and the factor $(-1)^{j_1+j_2-t}$ is a symmetry factor.¹³ As a quick check on this formalism, we can compute the coloured link invariant corresponding to the Hopf link using this method, and we find

$$\begin{aligned} \frac{\mathcal{S}_{ij}}{\mathcal{S}_{00}} &= \sum_{\ell=|i-j|}^{\text{Min}(i+j, k-i-j)} [2\ell+1] \lambda_{\ell, +}^{-2}(i, j) \\ &= \sum_{\ell=|i-j|}^{\text{Min}(i+j, k-i-j)} \left(\frac{q^{\ell+1/2} - q^{-\ell-1/2}}{q^{1/2} - q^{-1/2}} \right) q^{-i(i+1)-j(j+1)+\ell(\ell+1)} \\ &= \left(\frac{q^{-i(i+1)-j(j+1)}}{q^{1/2} - q^{-1/2}} \right) \sum_{\ell=|i-j|}^{\text{Min}(i+j, k-i-j)} \left(q^{(\ell+1)^2-1/2} - q^{\ell^2-1/2} \right) \\ &= \left(\frac{q^{-i(i+1)-j(j+1)}}{q^{1/2} - q^{-1/2}} \right) \left(q^{(\text{Min}(i+j, k-i-j)+1)^2-1/2} - q^{(i-j)^2-1/2} \right) \\ &= \left(\frac{q^{2ij+i+j+1/2} - q^{-2ij-i-j-1/2}}{q^{1/2} - q^{-1/2}} \right) \\ &= \frac{\sin\left(\frac{\pi(2i+1)(2j+1)}{k+2}\right)}{\sin\left(\frac{\pi}{k+2}\right)} \end{aligned} \quad (91)$$

which agrees with known results for the \mathcal{S} matrix of the $SU(2)_k$ WZW theory. (In the first line above we have used the formula

$$a_{0,l} \begin{pmatrix} j_1 & j_2 \\ j_3 & j_4 \end{pmatrix} = (-1)^{j_1+j_3-l} \sqrt{\frac{[2l+1]}{[2j_2+1][2j_3+1]}} \delta_{j_1, j_2} \delta_{j_3, j_4}. \quad (92)$$

¹³Note that [27] use eigenvalues which differ from ours by a phase factor. This factor is appended in their case to correct for the change in framing of the link arising from the braiding. But since we are interested in computing entanglement entropies, which as discussed previously are framing independent, we do not need to worry about these framing factors.

With these facts, we are now in a position to evaluate the Whitehead link invariant

$$\begin{aligned}
C_{5_1^2}(j_1, j_2) &= [2j_1 + 1]^2 [2j_2 + 1] \sum_{\mathbf{m}, \mathbf{n}, \mathbf{p}} \lambda_{p_1, -}^{-1}(j_1, j_2) \lambda_{p_2, +}(j_1, j_2) \lambda_{n_1, +}^{-1}(j_1, j_2) \lambda_{m_1, -}^{-1}(j_1, j_2) \lambda_{m_2, +}(j_1, j_2) \\
&\times a_{(\mathbf{0}, \mathbf{p})} \begin{pmatrix} j_1 & j_1 \\ j_2 & j_2 \\ j_1 & j_1 \end{pmatrix} a_{(\mathbf{n}, \mathbf{p})} \begin{pmatrix} j_1 & j_2 \\ j_1 & j_1 \\ j_2 & j_1 \end{pmatrix} a_{(\mathbf{n}, \mathbf{m})} \begin{pmatrix} j_1 & j_2 \\ j_1 & j_1 \\ j_2 & j_1 \end{pmatrix} a_{(\mathbf{0}, \mathbf{m})} \begin{pmatrix} j_1 & j_1 \\ j_2 & j_2 \\ j_1 & j_1 \end{pmatrix}
\end{aligned} \tag{93}$$

Similarly, we can also use the same techniques to evaluate the link invariant corresponding to the Borromean rings (figure 19). In this case, we find

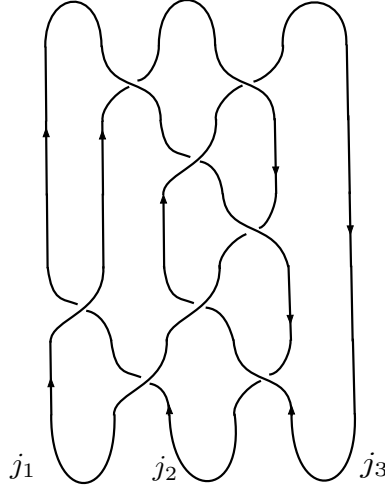


Figure 19: A plait representation for 6_2^3 , Borromean rings.

$$\begin{aligned}
C_{6_2^3}(j_1, j_2, j_3) &= \langle \phi_{\mathbf{0}}(\bar{j}_1, j_1, \bar{j}_2, j_2, \bar{j}_3, j_3) | B_2 B_4^{-1} B_1 B_3 B_4^{-1} B_3 B_2^{-1} B_4^{-1} | \phi_{\mathbf{0}}(j_2, \bar{j}_2, j_1, \bar{j}_1, j_3, \bar{j}_3) \rangle \\
&= [2j_1 + 1][2j_2 + 1][2j_3 + 1] \sum_{\mathbf{l}, \mathbf{m}, \mathbf{n}, \mathbf{p}, \mathbf{q}} \lambda_{l_1, -}(j_1, j_2) \lambda_{l_2, -}(j_1, j_3) \lambda_{m_1, -}^{-1}(j_2, j_3) \lambda_{n_2, +}^{-1}(j_1, j_2) \\
&\times \lambda_{p_0, +}(j_1, j_2) \lambda_{p_1, -}^{-1}(j_1, j_3) \lambda_{q_1, -}^{-1}(j_1, j_2) \lambda_{q_2, -}(j_2, j_3) \\
&\times a_{(\mathbf{0}, \mathbf{l})} \begin{pmatrix} j_2 & j_2 \\ j_1 & j_1 \\ j_3 & j_3 \end{pmatrix} a_{(\mathbf{m}, \mathbf{l})} \begin{pmatrix} j_2 & j_1 \\ j_2 & j_3 \\ j_1 & j_3 \end{pmatrix} a_{(\mathbf{m}, \mathbf{n})} \begin{pmatrix} j_2 & j_1 \\ j_3 & j_2 \\ j_1 & j_3 \end{pmatrix} \\
&\times a_{(\mathbf{p}, \mathbf{n})} \begin{pmatrix} j_2 & j_1 \\ j_3 & j_1 \\ j_2 & j_3 \end{pmatrix} a_{(\mathbf{p}, \mathbf{q})} \begin{pmatrix} j_1 & j_2 \\ j_1 & j_3 \\ j_2 & j_3 \end{pmatrix} a_{(\mathbf{0}, \mathbf{q})} \begin{pmatrix} j_1 & j_1 \\ j_2 & j_2 \\ j_3 & j_3 \end{pmatrix}
\end{aligned} \tag{94}$$

B Relative entropies of links

As mentioned in the body of the paper, the entanglement spectrum of a given link reduced on one or more of its components is a coarse measure of its topological properties. This is well illustrated particularly by the $2_1^2 + 2_1^2$ link depicted in Figure 11. Despite L_1 and L_2 playing very different roles in the link, the reduced density matrices $\rho_{L_1}(2_1^2 + 2_1^2)$ and $\rho_{L_2}(2_1^2 + 2_1^2)$ have identical spectrum. Additionally this spectrum is also found in a completely different link, 6_3^3 , depicted in Figure 12 reduced on one of its components. In these cases we expect relative entropy to provide a basis independent method to distinguish reduced density matrices. The relative entropy, $S(\rho||\sigma)$ is defined as:

$$S(\rho||\sigma) = \text{Tr}(\rho \ln \rho) - \text{Tr}(\rho \ln \sigma). \quad (95)$$

In this appendix we outline the two calculations of the relative entropy from the main text.

B.1 $2_1^2 + 2_1^2$

Let us begin with the two different ways of reducing the $2_1^2 + 2_1^2$ state: we can either trace over L_2 and L_3 or we can trace over L_1 and L_3 . We are interested in calculating $S(\rho_{L_1}||\rho_{L_2})$. Since $S_{EE}(\rho_{L_1|L_2,L_3})$ is known, what remains is the calculation of $\text{Tr}(\rho_{L_1} \ln \rho_{L_2})$. Tracing over L_2, L_3 gives the reduced density matrix

$$\rho_{L_1}(2_1^2 + 2_1^2) = n^{-1} \sum_j \sum_{ik} \frac{1}{|\mathcal{S}_{0j}|^2} \mathcal{S}_{ij} \mathcal{S}_{kj} |i\rangle \langle k|. \quad (96)$$

with normalization $n = \sum_j \frac{1}{|\mathcal{S}_{0j}|^2}$. Now we look at the reduced state from tracing over L_1, L_3 :

$$\rho_{L_2}(2_1^2 + 2_1^2) = n^{-1} \sum_j \frac{1}{|\mathcal{S}_{0j}|^2} |j\rangle \langle j|. \quad (97)$$

These expressions can more simply be written in terms of the orthonormal basis $|\hat{j}\rangle = \sum_i \mathcal{S}_{ij} |i\rangle$. From there, it is a simple matter to compute

$$\text{Tr}(\rho_{L_1} \ln \rho_{L_1}) = \sum_i p_i \ln p_i, \quad \text{Tr}(\rho_{L_1} \ln \rho_{L_2}) = \sum_{i,j} p_i |\mathcal{S}_{ij}|^2 \ln p_j \quad (98)$$

where we recall $p_j = \frac{d_j^{-2}}{\sum_i d_i^{-2}}$. The relative entropy between these two states is thus

$$S(\rho_{L_1}||\rho_{L_2}) = \sum_i p_i \left(\ln p_i - \sum_j |\mathcal{S}_{ij}|^2 \ln p_j \right) \quad (99)$$

It is straightforward to check that the relative entropy we obtained above is manifestly positive.¹⁴

B.2 6_3^3 vs. $2_1^2 + 2_1^2$

Now we comment on the spectrum of 6_3^3 and $2_1^2 + 2_1^2$ reduced on to a single component. In this case, it is useful to reduce 6_3^3 on L_2 yielding a reduced density matrix

$$\rho_{L_2}(6_3^3) = n^{-1} \sum_j \frac{1}{|\mathcal{S}_{0j}|^2} |\tilde{j}\rangle \langle \tilde{j}|. \quad (100)$$

with n the same as before, and we have introduced the orthonormal basis $|\tilde{j}\rangle \equiv \sum_m e^{-2\pi i h_m} \mathcal{S}_{mj} |m\rangle$. Now let us compare this to $2_1^2 + 2_1^2$ reduced on L_2 by computing $S(\rho_{L_2}(6_3^3) || \rho_{L_2}(2_1^2 + 2_1^2))$. We find

$$S(\rho_{L_2}(6_3^3) || \rho_{L_2}(2_1^2 + 2_1^2)) = \sum_i p_i \left(\ln p_i - \sum_j |\mathcal{S}_{ij}|^2 \ln p_j \right). \quad (101)$$

B.3 Distinguishability of two component links

For three component links the relative entropy is a useful way of comparing links with similar entanglement spectrum. For all of the two component links we considered above, their entanglement spectrum was enough to distinguish different links. A natural question one might want to consider in this context, however is whether the entanglement spectrum can characterize how different two links are; for simplicity let us consider how different a given link is from some fiducial simple link, for example the Hopf link, 2_1^2 . The natural tool to address this question is the relative entropy of links reduced on one of their components. In fact this question is particularly simple to address and the answer is that the distinguishability of the link is entirely encoded in its entanglement spectrum. To see this we note that 2_1^2 is the maximally mixed state:

$$\rho_{L_2|L_1}(2_1^2) = \frac{1}{\dim \mathcal{H}_{T_2}} \sum_i |i\rangle \langle i|. \quad (102)$$

Because of this, for any diagonalizable density matrix, $\tilde{\rho}_{L_2|L_1}$, on \mathcal{H}_{T_2} obtained by reducing a two component link on its second component,¹⁵ we can simultaneously diagonalize $\tilde{\rho}_{L_2|L_1}$ and $\rho_{L_2|L_1}(2_1^2)$. Let the spectrum of $\tilde{\rho}_{L_2|L_1}$ be $\{\tilde{p}_i\}_{i \in \text{span}(\mathcal{H}_{T_2})}$. Then it is a simple exercise to show that

$$S(\tilde{\rho}_{L_2|L_1} || \rho_{L_2|L_1}(2_1^2)) = -S(\tilde{\rho}) - \sum_i \tilde{p}_i \ln \left(\frac{1}{\dim \mathcal{H}_{T_2}} \right) = \ln(\dim \mathcal{H}_{T_2}) - S(\tilde{\rho}) \quad (103)$$

¹⁴One could also compute relative entropies of two component states obtained by tracing out one link. In some situations, this leads to infinite answers.

¹⁵In fact this argument works for any n component link reduced on $n - 1$ of its components $\tilde{\rho}_{L_1 \dots L_{n-1} | L_n}$.

where we used $\sum_i \tilde{p}_i = 1$. Therefore the distinguishability of a two component link from the Hopf link amounts to only knowing that link's entanglement spectrum.

References

- [1] W. Dur, G. Vidal, and J. I. Cirac, “Three qubits can be entangled in two inequivalent ways,” *Phys. Rev.* **A62** (2000) 062314.
- [2] V. Balasubramanian, P. Hayden, A. Maloney, D. Marolf, and S. F. Ross, “Multiboundary Wormholes and Holographic Entanglement,” *Class. Quant. Grav.* **31** (2014) 185015, [arXiv:1406.2663 \[hep-th\]](#).
- [3] D. Marolf, H. Maxfield, A. Peach, and S. F. Ross, “Hot multiboundary wormholes from bipartite entanglement,” *Class. Quant. Grav.* **32** (2015) no. 21, 215006, [arXiv:1506.04128 \[hep-th\]](#).
- [4] D. R. Brill, “Multi - black hole geometries in (2+1)-dimensional gravity,” *Phys. Rev.* **D53** (1996) 4133–4176, [arXiv:gr-qc/9511022 \[gr-qc\]](#).
- [5] S. Aminneborg, I. Bengtsson, D. Brill, S. Holst, and P. Peldan, “Black holes and wormholes in (2+1)-dimensions,” *Class. Quant. Grav.* **15** (1998) 627–644, [arXiv:gr-qc/9707036 \[gr-qc\]](#).
- [6] D. Brill, “Black holes and wormholes in (2+1)-dimensions,” [arXiv:gr-qc/9904083 \[gr-qc\]](#). [Lect. Notes Phys.537,143(2000)].
- [7] S. Aminneborg, I. Bengtsson, and S. Holst, “A Spinning anti-de Sitter wormhole,” *Class. Quant. Grav.* **16** (1999) 363–382, [arXiv:gr-qc/9805028 \[gr-qc\]](#).
- [8] K. Krasnov, “Holography and Riemann surfaces,” *Adv. Theor. Math. Phys.* **4** (2000) 929–979, [arXiv:hep-th/0005106 \[hep-th\]](#).
- [9] K. Krasnov, “Black hole thermodynamics and Riemann surfaces,” *Class. Quant. Grav.* **20** (2003) 2235–2250, [arXiv:gr-qc/0302073 \[gr-qc\]](#).
- [10] K. Skenderis and B. C. van Rees, “Holography and wormholes in 2+1 dimensions,” *Commun. Math. Phys.* **301** (2011) 583–626, [arXiv:0912.2090 \[hep-th\]](#).
- [11] S. Ryu and T. Takayanagi, “Holographic derivation of entanglement entropy from AdS/CFT,” *Phys. Rev. Lett.* **96** (2006) 181602, [arXiv:hep-th/0603001 \[hep-th\]](#).

- [12] E. Witten, “Quantum Field Theory and the Jones Polynomial,” *Commun. Math. Phys.* **121** (1989) 351–399.
- [13] E. Witten, “Topological Quantum Field Theory,” *Commun. Math. Phys.* **117** (1988) 353.
- [14] M. Atiyah, “Topological quantum field theories,” *Publications Mathématiques de l’Institut des Hautes Études Scientifiques* **68** (1988) no. 1, 175–186.
<http://dx.doi.org/10.1007/BF02698547>.
- [15] M. Marino, “Chern-Simons theory and topological strings,” *Rev. Mod. Phys.* **77** (2005) 675–720, [arXiv:hep-th/0406005](https://arxiv.org/abs/hep-th/0406005) [hep-th].
- [16] A. Kitaev and J. Preskill, “Topological entanglement entropy,” *Phys. Rev. Lett.* **96** (2006) 110404, [arXiv:hep-th/0510092](https://arxiv.org/abs/hep-th/0510092) [hep-th].
- [17] M. Levin and X.-G. Wen, “Detecting topological order in a ground state wave function,” *Phys. Rev. Lett.* **96** (Mar, 2006) 110405.
<http://link.aps.org/doi/10.1103/PhysRevLett.96.110405>.
- [18] S. Dong, E. Fradkin, R. G. Leigh, and S. Nowling, “Topological Entanglement Entropy in Chern-Simons Theories and Quantum Hall Fluids,” *JHEP* **05** (2008) 016, [arXiv:0802.3231](https://arxiv.org/abs/0802.3231) [hep-th].
- [19] A. Maloney and E. Witten, “Quantum Gravity Partition Functions in Three Dimensions,” *JHEP* **02** (2010) 029, [arXiv:0712.0155](https://arxiv.org/abs/0712.0155) [hep-th].
- [20] D. Rolfsen, *Knots and links*. Mathematics lecture series. Publish or Perish, 1976.
<https://books.google.com/books?id=qFLvAAAAMAAJ>.
- [21] D. Gepner and E. Witten, “String Theory on Group Manifolds,” *Nucl. Phys.* **B278** (1986) 493–549.
- [22] L. K. Hua, *Introduction to Number Theory*. Springer-Verlag Berlin Heidelberg, 1982.
- [23] K. Habiro, “On the colored Jones polynomials of some simple links,” *Surikaisekikenkyusho Kokyuroku* **1172** (2000) 34–43.
- [24] K. Habiro, “A unified Witten–Reshetikhin–Turaev invariant for integral homology spheres,” *Inventiones mathematicae* **171** (2008) , [arXiv:0605314](https://arxiv.org/abs/0605314) [math].
- [25] S. Gukov, S. Nawata, I. Saberi, M. Stosic, and P. Sulckowski, “Sequencing BPS Spectra,” *JHEP* **03** (2016) 004, [arXiv:1512.07883](https://arxiv.org/abs/1512.07883) [hep-th].

- [26] R. K. Kaul and T. R. Govindarajan, “Three-dimensional Chern-Simons theory as a theory of knots and links,” *Nucl. Phys.* **B380** (1992) 293–333, [arXiv:hep-th/9111063 \[hep-th\]](#).
- [27] R. K. Kaul, “Chern-Simons theory, colored oriented braids and link invariants,” *Commun. Math. Phys.* **162** (1994) 289–320, [arXiv:hep-th/9305032 \[hep-th\]](#).
- [28] R. K. Kaul, “Chern-Simons theory, knot invariants, vertex models and three manifold invariants,” in *Frontiers of field theory, quantum gravity and strings. Proceedings, Workshop, Puri, India, December 12-21, 1996*, pp. 45–63. 1998. [arXiv:hep-th/9804122 \[hep-th\]](#).
<http://alice.cern.ch/format/showfull?sysnb=0277169>.
- [29] E. Verlinde, “Fusion rules and modular transformations in 2d conformal field theory,” *Nuclear Physics B* **300** (1988) 360 – 376.
<http://www.sciencedirect.com/science/article/pii/0550321388906037>.
- [30] A. Peres, “Separability criterion for density matrices,” *Phys. Rev. Lett.* **77** (Aug, 1996) 1413–1415. <http://link.aps.org/doi/10.1103/PhysRevLett.77.1413>.
- [31] G. Vidal and R. F. Werner, “Computable measure of entanglement,” *Phys. Rev. A* **65** (Feb, 2002) 032314. <http://link.aps.org/doi/10.1103/PhysRevA.65.032314>.
- [32] M. Rangamani and M. Rota, “Entanglement structures in qubit systems,” *J. Phys.* **A48** (2015) no. 38, 385301, [arXiv:1505.03696 \[hep-th\]](#).
- [33] S. Eliahou, L. H. Kauffman, and M. B. Thistlethwaite, “Infinite families of links with trivial jones polynomial,” *Topology* **42** (2003) no. 1, 155 – 169.
<http://www.sciencedirect.com/science/article/pii/S0040938302000125>.
- [34] P. K. Aravind, *Borromean Entanglement of the GHZ State*, pp. 53–59. Springer Netherlands, Dordrecht, 1997. http://dx.doi.org/10.1007/978-94-017-2732-7_4.
- [35] L. H. Kauffman and S. J. L. Jr, “Quantum entanglement and topological entanglement,” *New Journal of Physics* **4** (2002) no. 1, 73. <http://stacks.iop.org/1367-2630/4/i=1/a=373>.
- [36] A. Sugita, “Borromean Entanglement Revisited,” [arXiv:0704.1712v1](#).
- [37] A. I. Solomon and C. L. Ho, “Links and Quantum Entanglement,” [arXiv:1104.5144v1](#).
- [38] R. M. Kashaev, “The Hyperbolic volume of knots from quantum dilogarithm,” *Lett. Math. Phys.* **39** (1997) 269–275.
- [39] S. Gukov, “Three-dimensional quantum gravity, Chern-Simons theory, and the A polynomial,” *Commun. Math. Phys.* **255** (2005) 577–627, [arXiv:hep-th/0306165 \[hep-th\]](#).

- [40] T. Dimofte and S. Gukov, “Quantum Field Theory and the Volume Conjecture,” *Contemp. Math.* **541** (2011) 41–67, [arXiv:1003.4808 \[math.GT\]](#).
- [41] G. Salton, B. Swingle, and M. Walter, “Entanglement from Topology in Chern-Simons Theory,” [arXiv:1611.01516 \[quant-ph\]](#).
- [42] G. W. Moore and N. Seiberg, “Classical and Quantum Conformal Field Theory,” *Commun. Math. Phys.* **123** (1989) 177.